Supporting Information for

3D Cage COFs: A Dynamic Three-Dimensional Covalent Organic Framework with High-Connectivity Organic Cage Nodes

Qiang Zhu,[†] Xue Wang,[†‡] Rob Clowes,[†] Peng Cui,[†] Linjiang Chen,[*†‡] Marc A. Little,[*†] Andrew I. Cooper[*†‡]

†Department of Chemistry and Materials Innovation Factory, University of Liverpool, Liverpool, L7 3NY, UK.

‡Leverhulme Research Centre for Functional Materials Design, University of Liverpool, Liverpool, L7 3NY, UK.

Contents

Section 1 Materials and Methods....2

Section 2 General Synthetic Procedures....4

Section 3. Screening of **3D-CageCOF-1** Synthetic Conditions....11

Section 4 Gas Sorption Isotherms for **3D-CageCOF-1** 16

Section 5 Structural Modelling for **3D-CageCOF-1**....25

Section 6 Scanning Electronic Microscopy and Transmission Electron Microscopy Images for **3D-CageCOF-1** 31

Section 7 Fourier-transform Infrared Spectra and Solid-State NMR Spectrum for **3D-CageCOF-1** 32

Section 8 Thermogravimetric Analysis and Solid-state UV-vis Spectra for **3D-CageCOF-1** 34

Section 9 Stability Tests for **3D-CageCOF-1** 36

Section 10 Characterization of Dynamic Behaviour of **3D-CageCOF-1** 38

Section 11 Single Crystal X-ray Diffraction Data for Cage-6-NO_2 and Model Compound 39

Section 12 Atomic Coordinates and Unit Cell Parameters of **sp** Model and **lp** Model for 3**D-CageCOF-1** 43

Reference 47

Section 1 Materials and Methods

General Methods

All reagents were obtained from Sigma-Aldrich, TCI Europe, Fisher, Manchester Organics, Alfa Aesar, and Yanshen Technology and used as received. Anhydrous solvents were purchased from Acros Organics and used without further purification. All gases for sorption analysis were supplied by BOC at a purity of ≥99.9%. Reactions were carried out under nitrogen atmosphere using standard Schlenk techniques.

NMR

NMR spectra were recorded on a Bruker 400 NMR spectrometer at 400 MHz (^{1}H) and 100 MHz (^{13}C) and referenced against the residual ^{1}H or ^{13}C signal of the solvent.

Powder X-ray Diffraction (PXRD)

Laboratory powder X-ray diffraction (PXRD) data patterns were collected in transmission mode on samples held on thin Mylar film in aluminium well plates on a Panalytical Empyrean diffractometer equipped with a high throughput screening (HTS) XYZ stage, X-ray focusing mirror, and PIXcel detector, using Cu-Kα radiation. For HT screening, PXRD patterns were measured over the 2θ range 2-40° in 0.013° steps over 30 minutes. Capillary PXRD patterns were collected on powdered samples loaded in borosilicate glass capillaries that were spun to improve averaging. For the capillary measurements recorded as suspensions in DMF, a small portion of DMF (5 ul) was dropped into a glass capillary containing a powdered sample of activated **3D-CageCOF-1** at room temperature. The capillary was then heated from room temperature to 175 °C using an Oxford Cryosystems 700 series cryostream. An equilibration time of 1 hour was used at each temperature set point.

Single Crystal X-ray Diffraction (SC-XRD)

Single crystal X-ray data for **Cage-6-NO$_2$** was measured on a Rigaku MicroMax-007 HF rotating anode diffractometer (Mo-Kα radiation, λ = 0.71073 Å, Kappa 4-circle goniometer, Rigaku Saturn724+ detector) and data reduction was performed using CrysAlisPro. Single crystal data for the **model compound** was measured at beamline I19, Diamond Light Source, Didcot, UK using silicon double crystal monochromated synchrotron radiation (λ = 0.6889 Å, Pilatus 2M detector) and data reduction was performed using xia2. Structures were solved with SHELXT[1] and refined by full-matrix least-squares on $|F|^2$ by SHELXL,[2] interfaced through the programme OLEX2.[3] All non-H atoms were refined anisotropically and all H-atoms were fixed in geometrically estimated positions and refined using the riding model. For full refinement details, see Tables S4-5.

Fourier-transform infrared spectroscopy

FT- IR spectra were recorded using a Bruker Tensor 27 FT-IR spectrometer using KBr disks.

Solid State NMR

Solid-state NMR experiments were performed on a Bruker Avance III HD spectrometer using the Durham University (UK) solid-state NMR service. The^{13}C CP/MAS NMR spectra were recorded with a 4-mm MAS probe and with a sample spinning rate of 8.0 kHz.

Gas Sorption Analysis

Surface areas were measured by nitrogen sorption at 77.3 K. Powder samples were degassed offline, followed by degassing on the analysis port under vacuum at 120 °C for 15 hours. Isotherm measurements were performed using a Micromeritics 3flex surface characterization analyser, equipped with a Cold-Edge technologies liquid helium cryostat chiller unit for temperature control. CO_2 and CH_4 sorption were measured with the same procedure at 273 K and 298 K, using a Micromeritics ASAP

2020 characterization analyser. H_2 sorption was measured with the same procedure at 77 K, using a Micromeritics ASAP 2020 characterization analyser.

Water vapor sorption

Water vapor sorption isotherms were measured at 298 K and 313 K using an IGA gravimetric adsorption apparatus (Hiden Isochema, Warrington, UK) fitted with an anti-condensation system, which was carried out in an ultrahigh vacuum system equipped with a diaphragm and turbopumps.

Thermogravimetric analysis (TGA)

TGA analysis was carried out using a TA Q5000IR analyzer with an automated vertical overhead thermobalance. Samples were heated at a rate of 10 °C/min under a dry nitrogen gas flow.

Differential scanning calorimetry analysis (DSC)

DSC measurements were carried out on a TA Q2000 instrument with a Refrigerated Cooling System 90 and an auto sampler). The sample was heated in a sealed pan at a rate of 20 °C/min from 30 °C to 400 °C.

Scanning electron microscopy (SEM)

SEM images were recorded using a Hitachi S-4800 cold field emission scanning electron microscope (FE-SEM). Samples were prepared by depositing the dry powders on a silicon disk and then coating the samples with Chromium using an Emitech K550X automated sputter coater. Imaging was conducted at a working voltage of 3 kV and a working distance of 8 mm using a combination of upper and lower secondary electron detectors.

Transmission electron microscopy (TEM)

Transmission electron microscopy images were collected using a JEOL JEM-2100 TEM equipped with a thermal LaB_6 gun, operated at an acceleration voltage of 200 kV. The images were recorded using a Gatan Orius SC200D CCD camera.

Section 2 General Synthetic Procedures

4,6,16,18,31,33-hexanitro-2,8,14,20,29,35-hexaoxabicyclocalix[4]arene (Cage-6-NO_2)

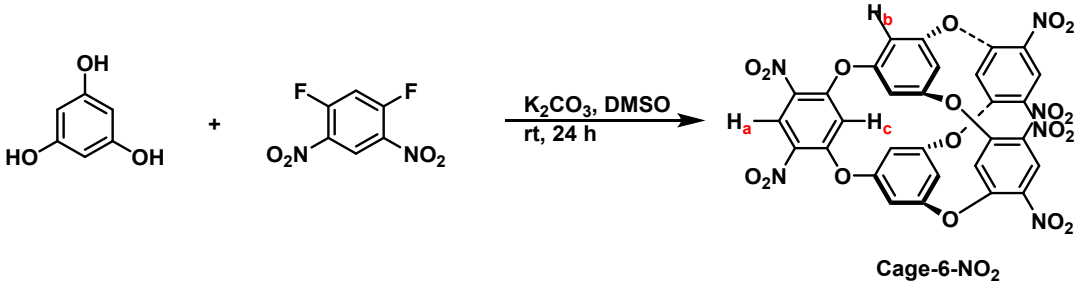

Scheme S1 synthesis of Cage-6-NO_2

Cage-6-NO_2 was synthesized according to a reported procedure with some modifications.[4]
To a mixture of phloroglucinol (410 mg, 3.3 mmol) and 1,5-difluoro-2,4-dinitrobenzene (1 g, 5.0 mmol) in DMSO (50 mL), ground K_2CO_3 (1.7 g) was added. The reaction was stirred at room temperature for 24 hours. The reaction mixture was then poured onto 1 M HCl (200 mL) and the resulting suspension was stirred for another 30 mins. The solid was then collected by filtration and washed with water. The solid was collected and washed with acetone (10 mL x 3), and MeOH (10 mL x 3). The pure product was obtained after removing the solvent under vacuum at room temperature to afford **Cage-6-NO_2** in a yield of 890 mg: 73%. A single crystal of **Cage-6-NO_2** was grown from a solvent mixture of CH_3CN and acetone.

^{1}H NMR (DMSO-d_6, 400 MHz): δ = 8.99 (s, 3H_a), 7.56 (s, 6H_b), 5.53 (s, 3H_c). ^{13}C NMR (DMSO-d_6, 100 MHz): δ = 156.63, 155.77, 132.17, 126.52, 117.71, 104.88. (signals at 170.81, 60.22, 21.24, 14.56 were assigned to ethyl acetate solvent). All spectroscopic data was consistent with literature reported data.[4]

4,6,16,18,31,33-hexamino-2,8,14,20,29,35-hexaoxabicyclocalix[4]arene (Cage-6-NH_2)

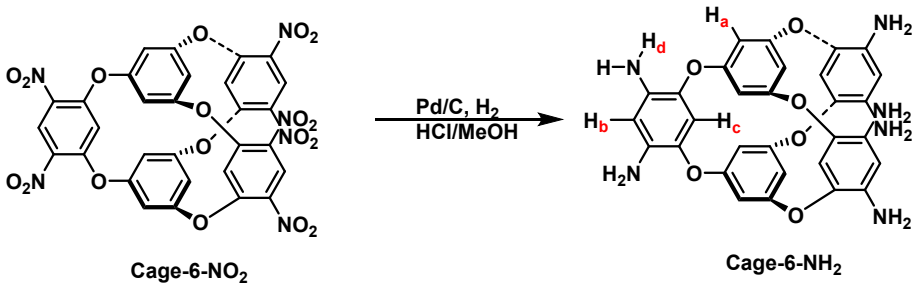

Scheme S2 synthesis of **Cage-6-NH_2**

To a nitrogen degassed solution of Cage-6-NO_2 (600 mg, 0.81 mmol) and 10 wt% wet Pd/C (120 mg) in 50 mL MeOH, hydrochloride MeOH solution was added (1.25M, 10 mL). The reaction was degassed with nitrogen and then H_2, before being left to stir at room temperature for 48 hours under H_2 atmosphere. After the reaction, Pd/C was removed by filtration using *Celite* that was washed with MeOH. The filtrate was concentrated to 5 mL and then NEt_3 (3 mL) was added. The filtrate was collected by filtration, washed with MeOH, and dried under vacuum, to afford pure **Cage-6-NH_2** as a grey solid in a yield of 88 mg (0.16 mmol): 20%.

^{1}H NMR (DMSO-d_6, 400 MHz): δ = 6.52 (s, 6H_a), 6.16 (s, 3H_b), 5.17 (s, 3H_c), 4.51 (s, 12H_d).

^{13}C NMR (DMSO-d_6, 100 MHz): δ = 159.00, 139.47, 132.49, 116.03, 103.65, 103.04. (signals at 56.49 and 19.01 was assigned to ethanol solvent).
MS-ESI (m/s) $[M+H]^+$, $[C_{30}H_{20}N_6O_6+H]$: Calc. 565.183, Found 565.1827.

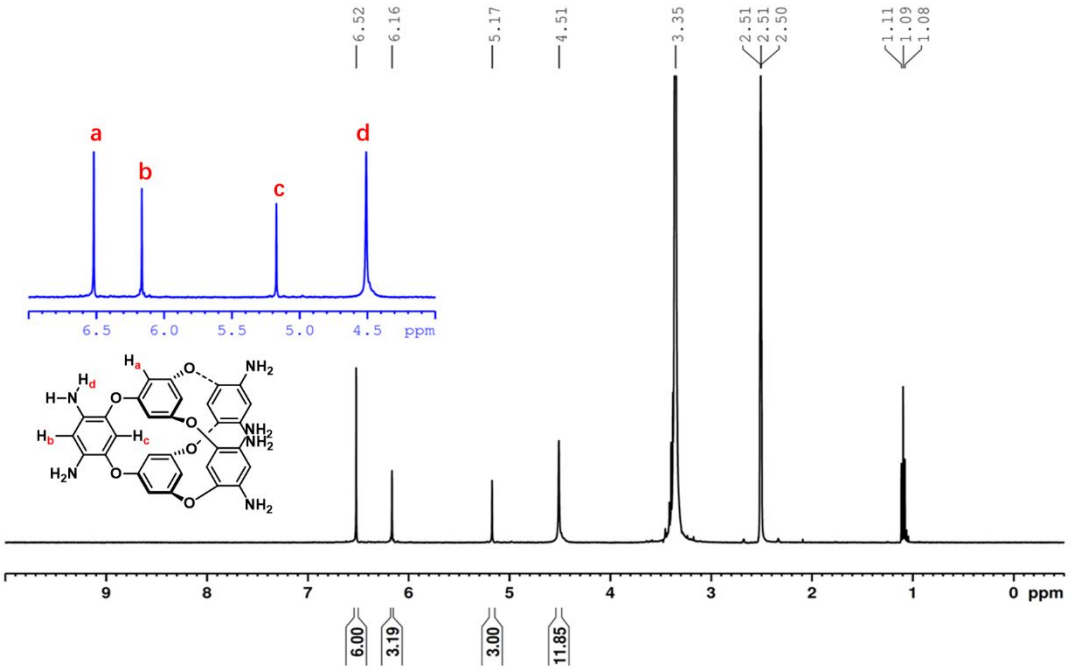

Figure S1 ^{1}H NMR (400 MHz, DMSO-d_6) spectrum of **Cage-6-NH$_2$**. In the ^{1}H spectrum, there are only four sharp singlets for **Cage-6-NH$_2$** (see insert, H_a, H_b, H_c, and H_d) because the three cage arms are equivalent and that the two 1,3,5-substituted aromatic rings are equivalent. The ^{1}H NMR, therefore, indicates that **Cage-6-NH$_2$** has a principal C_3 axis, three equivalent C_2 axes perpendicular to the C_3 axis, and a mirror plane perpendicular to the C_3 axis, which corresponds to **Cage-6-NH$_2$** having D_{3h} symmetry, which is comparable to the symmetry of the previously reported hexa-nitro precursor.[4]

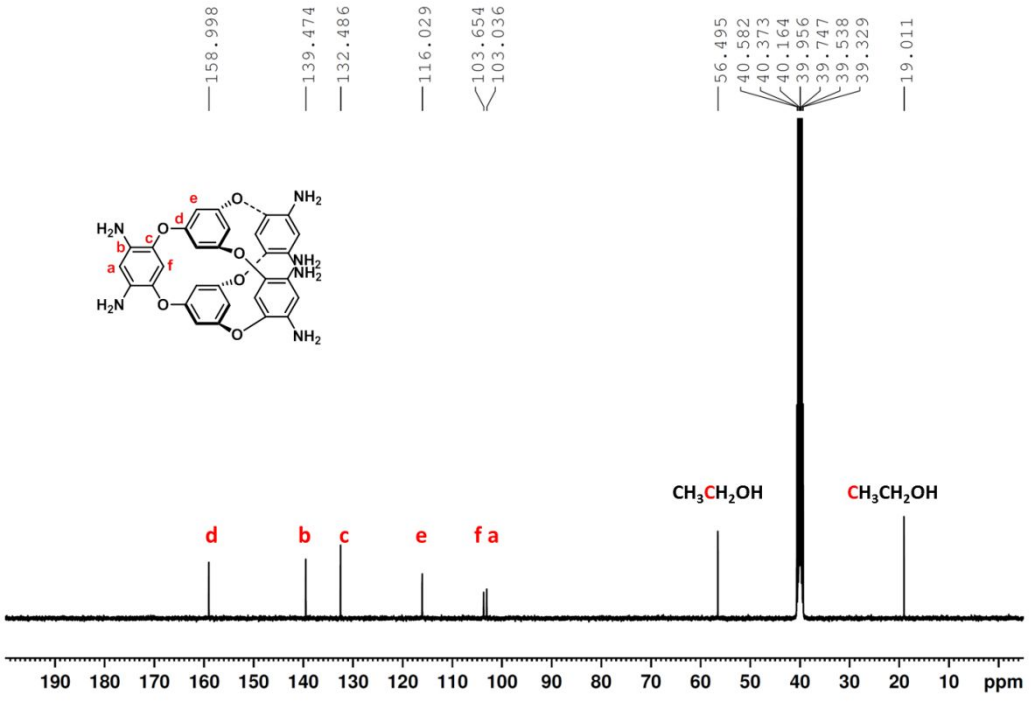

Figure S2 ^{13}C NMR (100 MHz, DMSO-d_6) spectrum of **Cage-6-NH$_2$**.

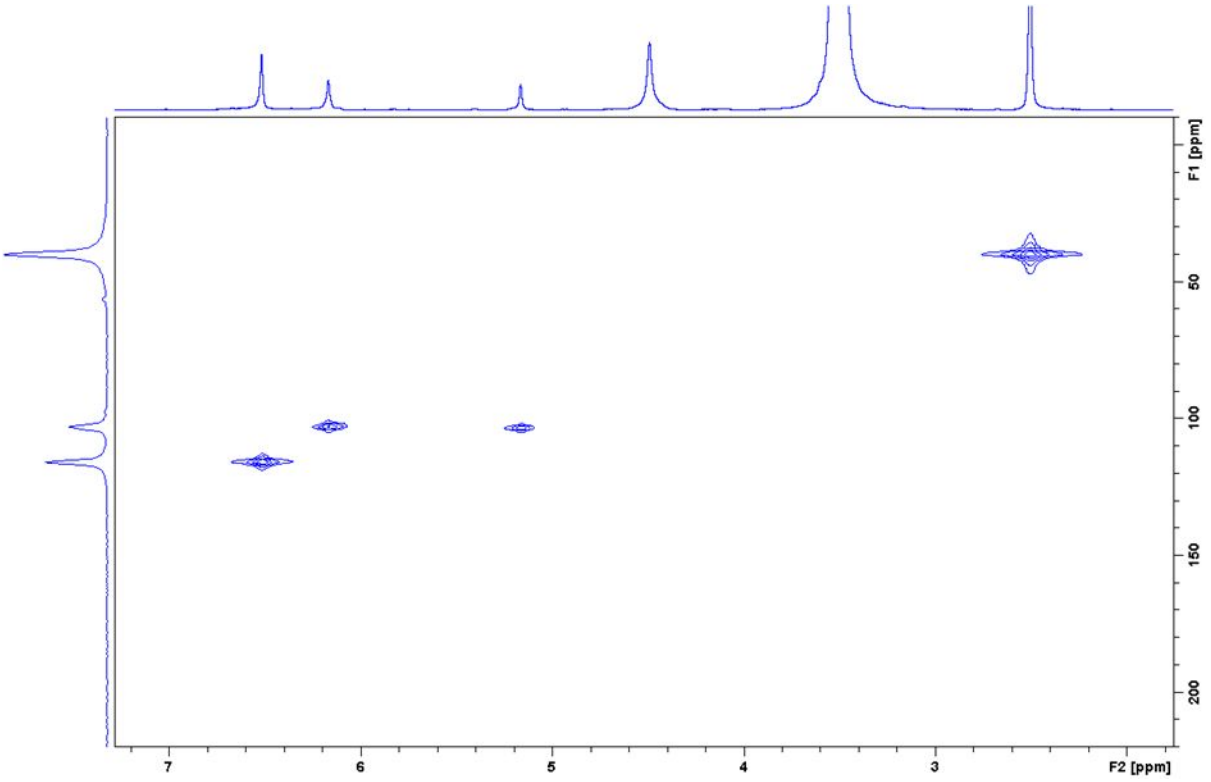

Figure S3 HSQC (DMSO-d_6) spectrum of **Cage-6-NH_2**

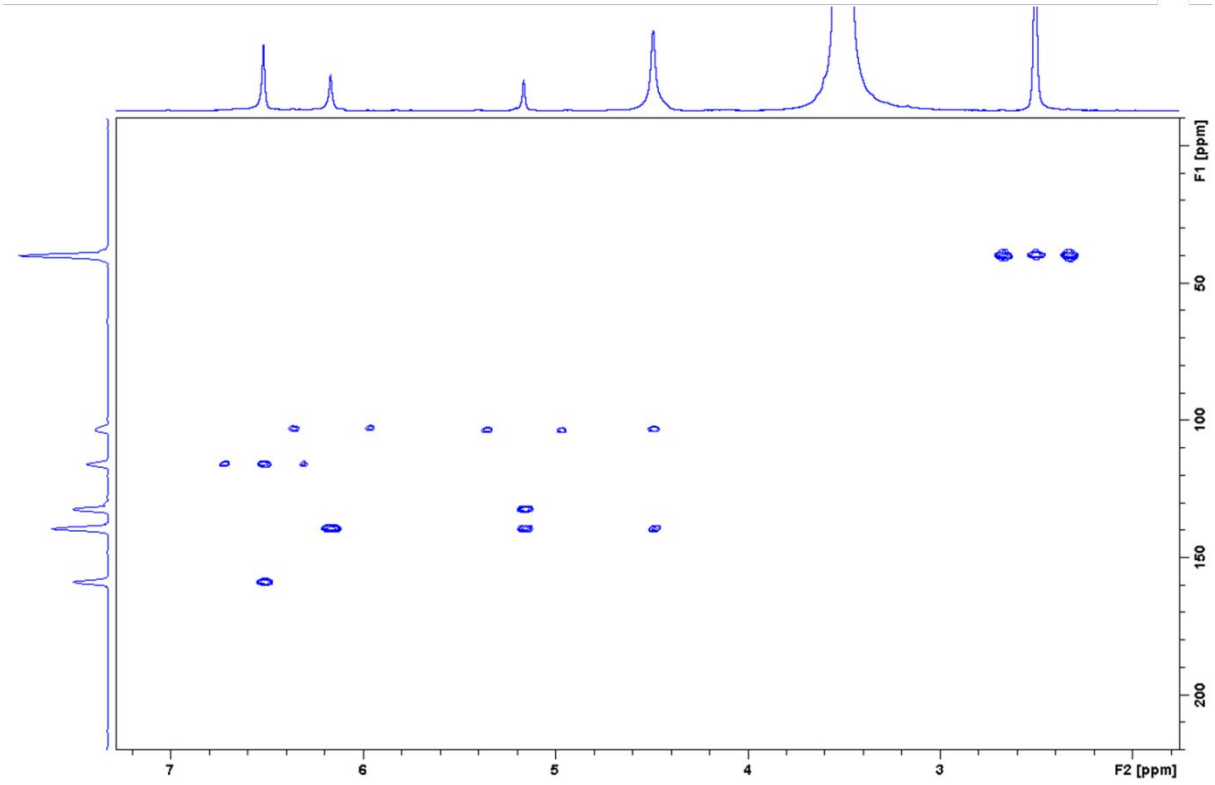

Figure S4 HMBC (DMSO-d_6) spectrum of **Cage-6-NH_2.**

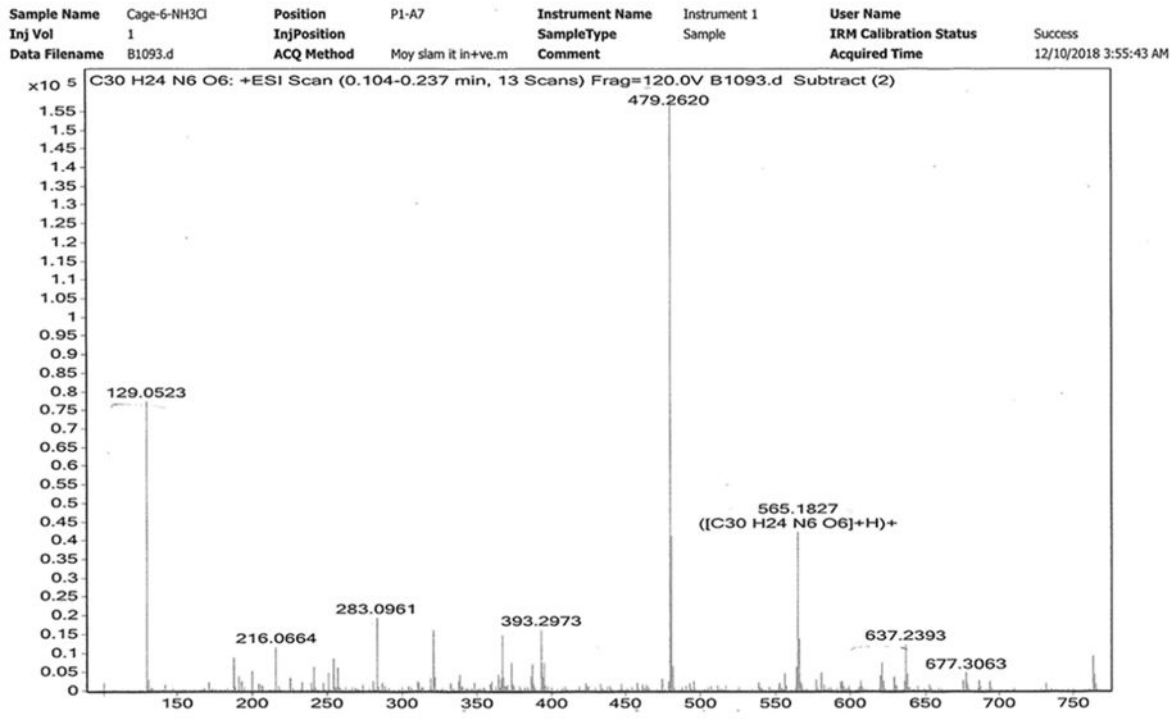

Figure S5 MS $[M+H]^+$ spectrum of **Cage-6-NH_2.**

2,5-dihydroxyterephthalaldehyde (DHTPA)

Scheme S3 synthesis of DHTPA

2,5-dihydroxyterephthalaldehyde was synthesized according to a previously reported procedure.[5]
To a solution of 2,5-dimethoxyterephthalaldehyde (1 g, 4 mmol) in anhydrous dichloromethane (100 mL), BBr_3 (6.44 mL, 1 M in hexane) was added dropwise at 0 °C under N_2 atmosphere. After stirring the reaction at room temperature overnight, the reaction was slowly quenched with water. The solid was collected by filtration and washed with water and dichloromethane. The filtrate was extracted with dichloromethane, washed with brine, dried over Na_2SO_4, and the solvent was evaporated under reduced pressure to afford the crude compound. The crude compound was purified by the recrystallization with EtOAc to afford DHTPA in a yield of 780 mg: 91%.
^{1}H NMR (DMSO-d_6, 400 MHz): δ = 10.36 (s, 2H$_a$), 10.30 (s, 2H$_b$), 7.22 (s, 2H$_c$).
^{13}C NMR (DMSO-d_6, 100 MHz): δ = 19.69, 153.24, 128.10, 116.03, 115.56, 103.65.

Synthesis of Model Compound 1

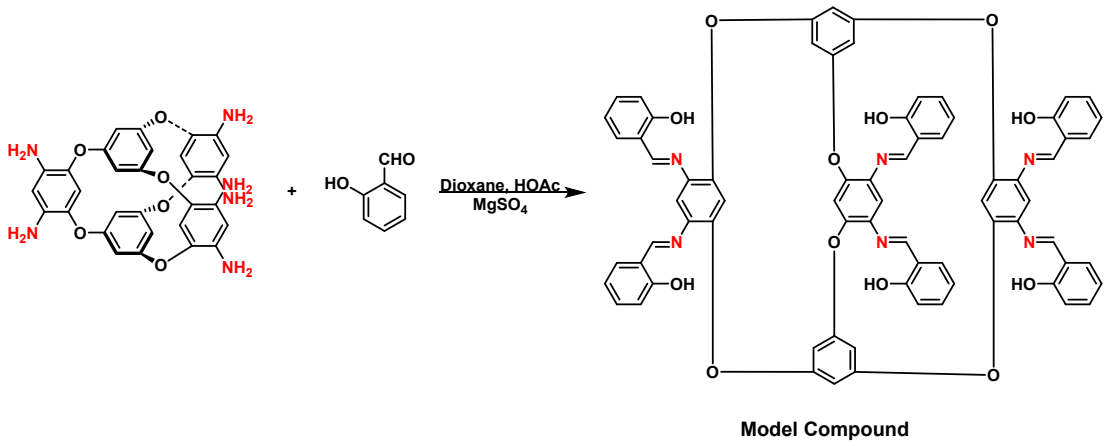

Scheme S4 synthesis of the model compound.

To a mixture of **Cage-6-NH$_2$** (0.06 mmol, 32.4 mg) and acetic acid (0.4 ml, 6 M) in 1,4-dioxane (4 mL) 2-hydroxybenzaldehyde (112 uL, 1.07 mmol) was added. The reaction mixture was then stirred under an N_2 atmosphere for 24 hours. The resulting solid was then separated by filtration and washed with EtOH and diethyl ether to afford the model compound in a yield of 50 mg: 70%. Single crystals of the model compound that were suitable for X-ray diffraction were grown by slowly diffusing diethyl ether into a toluene solution.

^{1}H NMR (DMSO-d_6, 400 MHz): δ = 13.50 (s, 6H$_a$), 9.20 (s, 6H$_b$), 7.95 (s, 3H$_c$), 7.65 (d, 6 H$_d$), 7.43(t, 6H$_e$), 7.28 (s, 6H$_f$), 7.02-6.96 (s, 12 H$_g$, H$_f$), 5.59 (s, 3H$_i$).

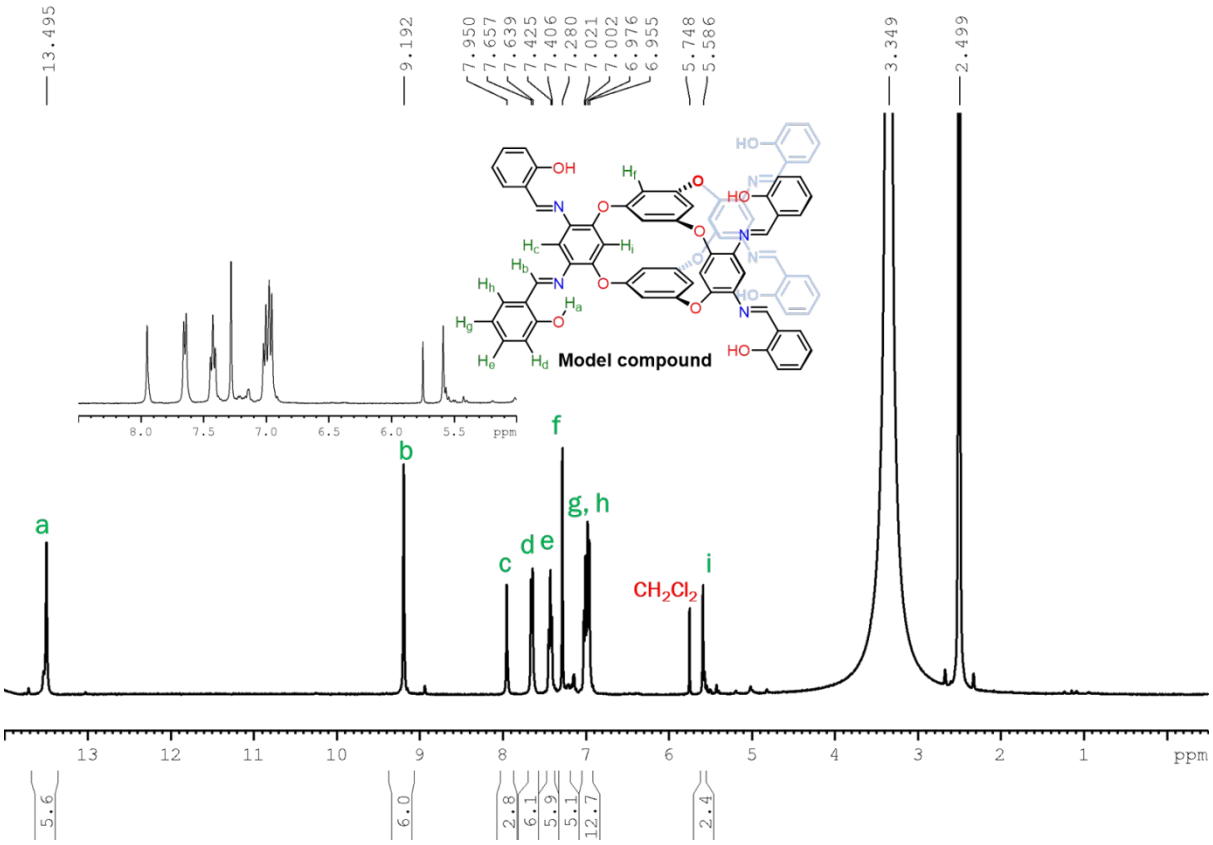

Figure S6 ^{1}H NMR (400 MHz, DMSO-d_6) spectrum of the **model compound**.

General Procedure used to Synthesis 3D-CageCOF-1

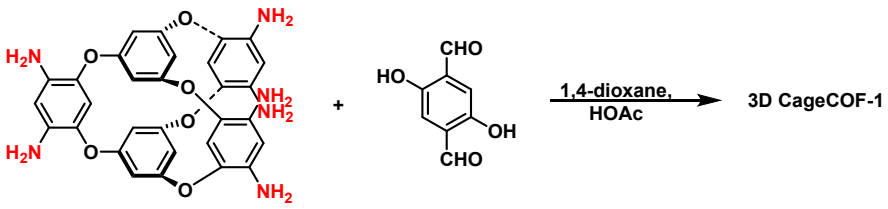

Scheme S5 synthesis of **3D-CageCOF-1**

To a mixture of 2,5-dihydroxyterephthalaldehyde (0.09 mmol, 14.9 mg), aniline (20.5 uL), HOAc (6M, 0.1 mL) in 1,4-dioxane (1 mL), **Cage-6-NH$_2$** (0.03 mmol, 16.2 mg) was added and the reaction mixture was sonicated for 1 min. The Pyrex tube was then flash frozen in a liquid nitrogen bath, evacuated under vacuum, and sealed. The tube was warmed to room temperature and then placed in an oven that was heated at 120 °C for between 3-7 days. Afterward, the solid was isolated by filtration, washed with DMF and acetone, and dried in the air, before being subjected to PXRD characterization. Further purification was carried out by Soxhlet using THF or acetone solvent.

Table S1 Synthetic conditions that were screened for synthesizing **3D-CageCOF-1**.

Entry	Solvent 1 (mL)	Solvent 2 (mL)	Catalyst (conc., mL)	Aniline (ul)	T (°C)	T (days)	Crystallinity
1	NMP (1.0)	——	HOAc (6M, 0.1)	—	120	3	poor
2	Diox (1.0)	——	HOAc (6M, 0.1)	—	120	3	amorphous
3	o-DCB (1.0)	——	HOAc (6M, 0.1)	—	120	3	amorphous
4	n-BuOH (1.0)	——	HOAc (6M, 0.1)	—	120	3	amorphous
5	NMP (0.7)	MES (0.3)	HOAc (6M, 0.1)	—	120	3	poor
6	NMP (0.5)	MES (0.5)	HOAc (6M, 0.1)	—	120	3	poor
7	NMP (0.8)	MES (0.2)	HOAc (6M, 0.1)	—	120	3	amorphous
8	NMP (0.7)	MES (0.3)	HOAc (3M, 0.1)	—	120	3	poor
9	NMP (0.7)	MES (0.3)	HOAc (9M, 0.1)	—	120	3	poor
10	NMP (0.7)	MES (0.3)	HOAc (12M, 0.1)	—	120	3	poor
11	NMP (0.7)	MES (0.3)	HOAc (0.1)	—	120	3	amorphous
12	NMP (0.7)	MES (0.3)	CF_3COOH (3M, 0.1)	—	120	3	amorphous
13	1,4-Dioxane (1.0)	——	HOAc (6M, 0.1)	12.3	120	3	poor
14	1,4-Dioxane (1.0)	——	HOAc (6M, 0.1)	16.4	120	3	high
15	1,4-Dioxane (1.0)	——	HOAc (6M, 0.1)	20.5	120	3	high
16	1,4-Dioxane (1.0)	——	HOAc (6M, 0.1)	41	120	3	poor
17	1,4-Dioxane (1.0)	——	HOAc (6M, 0.1)	164	120	3	poor
18	1,4-Dioxane (1.0)	——	HOAc (6M, 0.1)	328	120	3	oligomers
19	1,4-Dioxane (1.0)	——	HOAc (6M, 0.1)	20.5	RT	3	oligomers
20	1,4-Dioxane (1.0)	——	HOAc (6M, 0.1)	20.5	80	3	high
21	1,4-Dioxane (1.0)	——	HOAc (6M, 0.1)	20.5	100	3	high
22	1,4-Dioxane (1.0)	——	HOAc (6M, 0.1)	20.5	120	3	poor[a]
23	1,4-Dioxane (1.0)	——	HOAc (6M, 0.1)	20.5	150	3	poor
24	1,4-Dioxane (1.0)	——	HOAc (3M, 0.1)	20.5	120	3	high
25	1,4-Dioxane (1.0)	——	HOAc (9M, 0.1)	20.5	120	3	high
26	1,4-Dioxane (1.0)	——	HOAc (6M, 0.2)	20.5	120	3	high
27	1,4-Dioxane (1.0)	——	$Sc(OTf)_3$ (0.18M, 0.1)	20.5	120	3	poor
28	1,4-Dioxane (1.0)	——	$Sc(OTf)_3$ (0.36M, 0.1)	20.5	120	3	poor

[a]performed under an Ar atmosphere.

Section 3. Screening of 3D-CageCOF-1 Synthetic Conditions

Optimization of reaction solvent

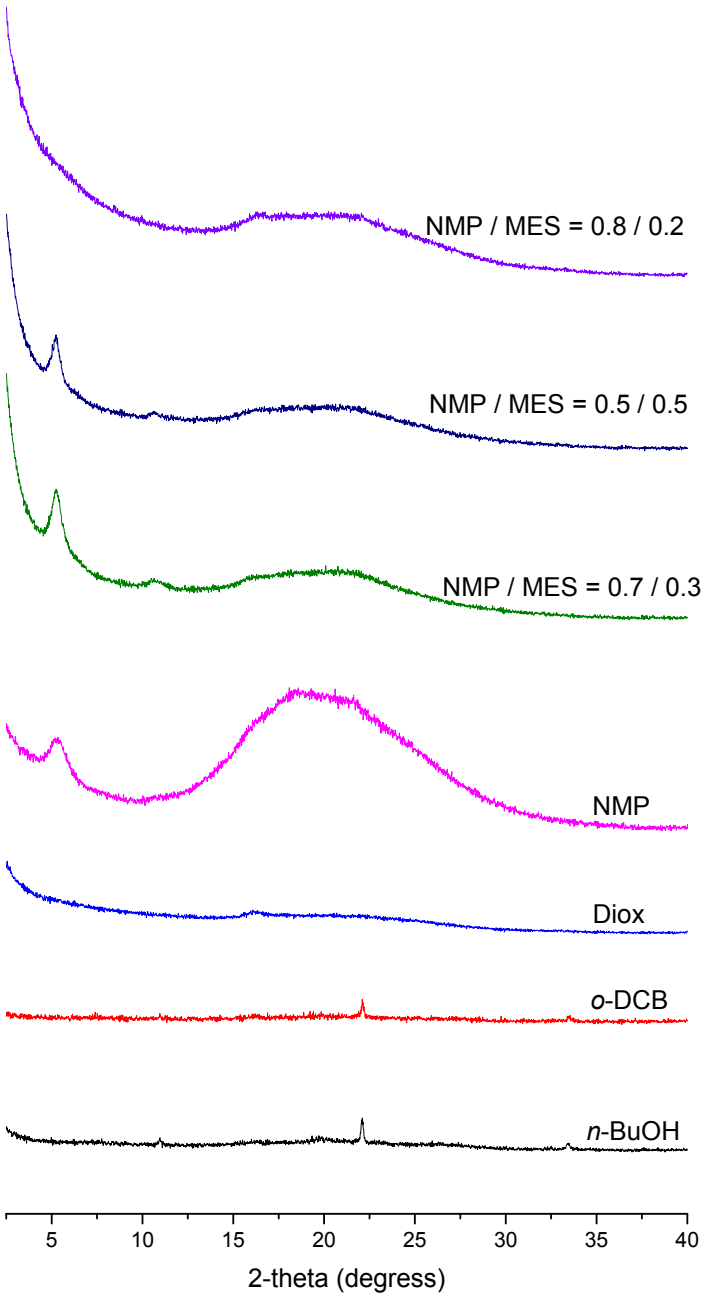

Figure S7 PXRD patterns for dried powdered samples that were synthesized using the different reaction solvents, *n*-butyl alcohol (n-BuOH), *o*-dichlorobenzene (*o*-DCB), 1,4-dioxane (Diox), *N*-Methylpyrrolidone (NMP) and mesitylene (MES). HOAc (6 M, 0.1 mL) was used as the catalyst and the reactions were all heated at 120 °C for 3 days.

Optimization of acid catalyst

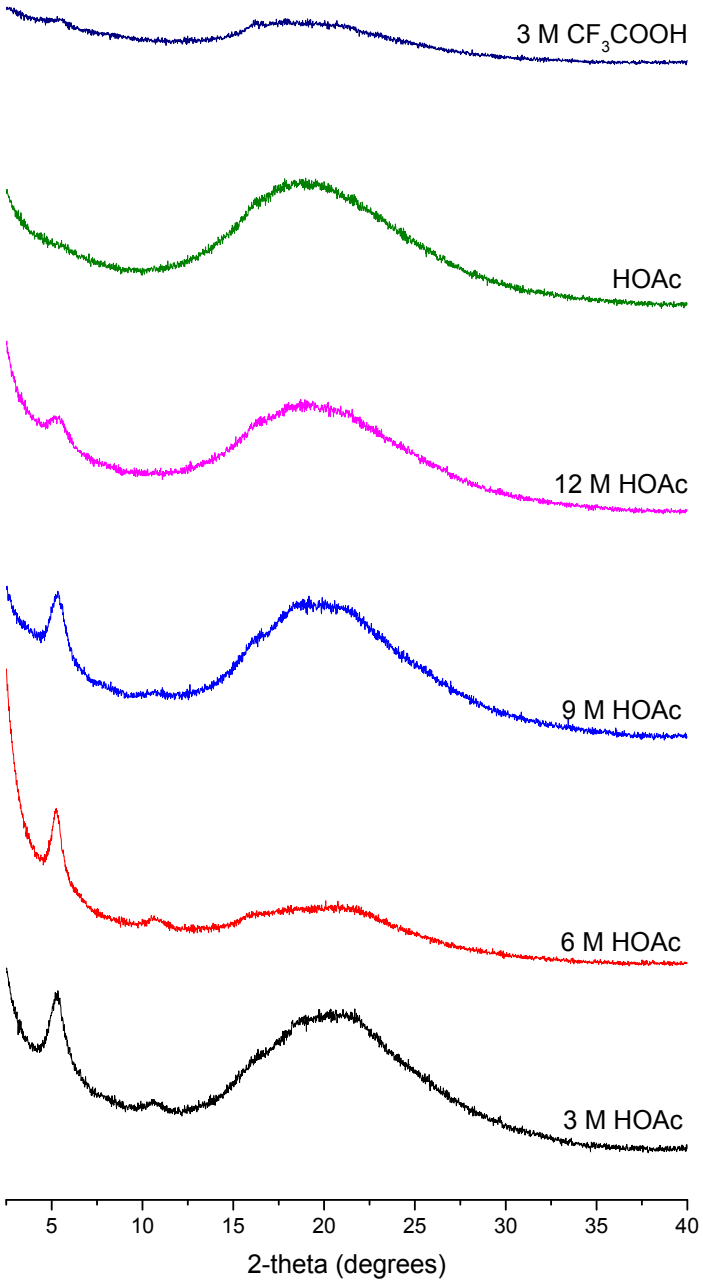

Figure S8 PXRD patterns for dried powdered samples that were synthesized using different acid catalyst conditions. All the reactions were carried out using the same solvent mixture (NMP: 0.7 mL, MSE: 0.3 mL) and heated at 120 °C for 3 days.

Optimization of aniline concentration

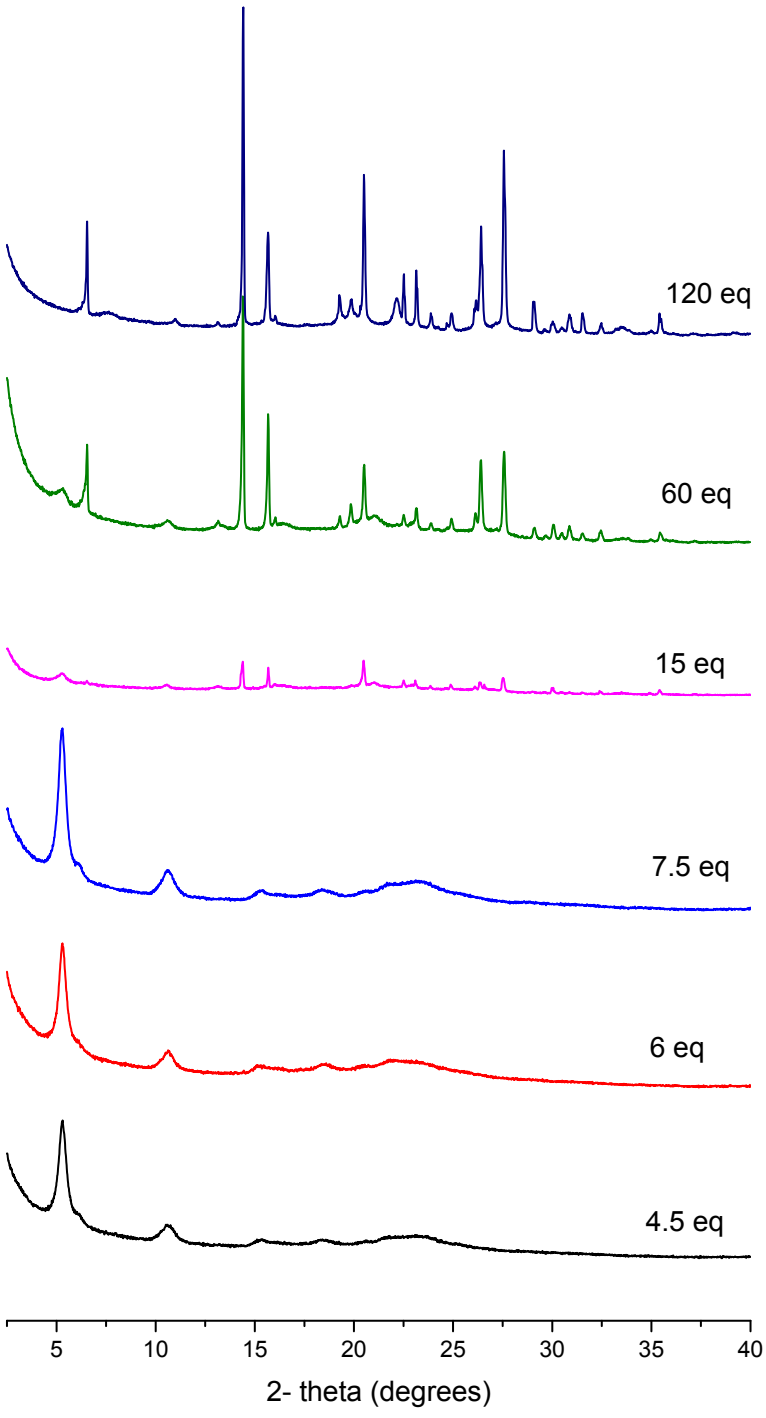

Figure S9 PXRD patterns for dried powdered samples of **3D-CageCOF-1** that were synthesized using different concentrations of aniline (4.5-120 eq. based on the molar concentration of **Cage-6-NH_2**). All of the reactions were carried out using the same synthesis conditions: dioxane (1.0 mL), HOAc (6 M, 0.1 mL), reaction temperature = 120 °C, reaction time = 3 days, and the PXRD patterns were collected after washing the reaction filtrate with acetone and drying the samples in air.

Optimization of reaction temperature using 7.5 equivalents of aniline

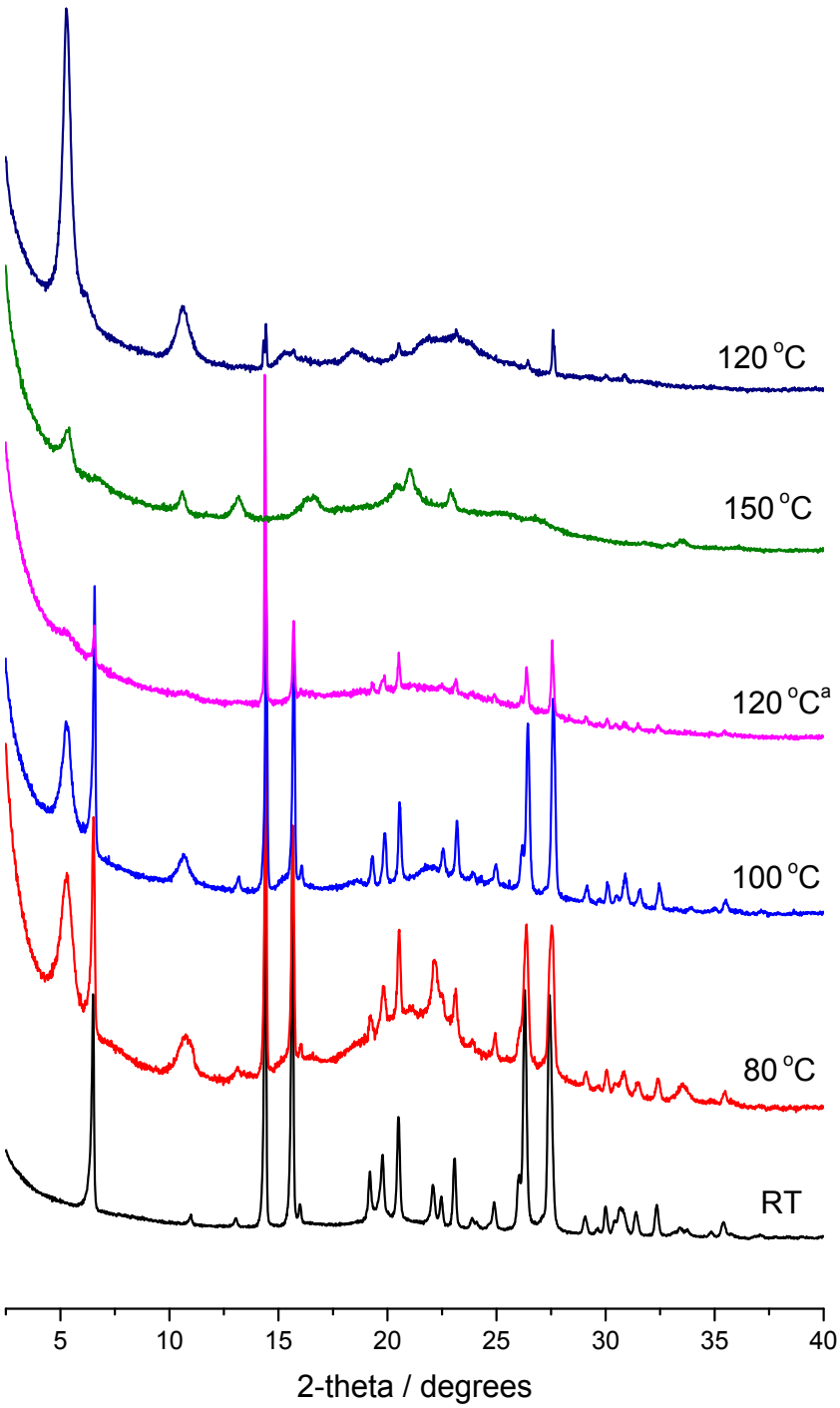

Figure S10 PXRD patterns for **3D-CageCOF-1** samples that were synthesized using different reaction temperatures. All the reactions were carried out using the same solvent mixture: dioxane (1.0 mL), aniline (20.5 uL), HOAc (6 M, 0.1 mL), and a reaction time of 3 days. The PXRD patterns were recorded after washing the reaction filtrate with acetone and drying the samples in air. [a]Synthesized under an Ar atmosphere.

Optimizing of the acid conditions with aniline

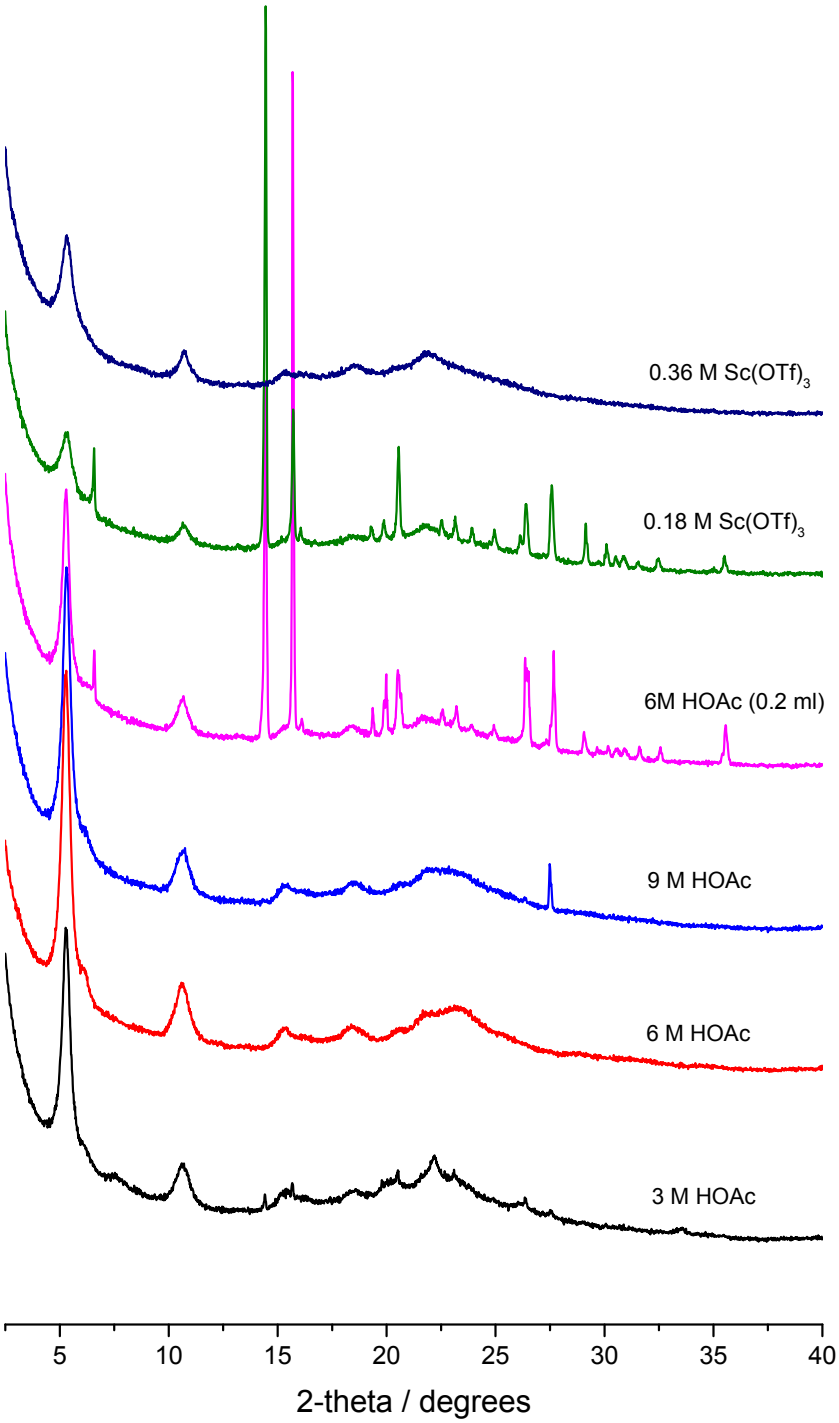

Figure S11 PXRD patterns for **3D-CageCOF-1** samples that were synthesized using different acid catalysts. All the reactions were carried out using the same solvent mixture: dioxane (1.0 mL), aniline (20.5 uL), a reaction temperature of 120 °C, and a reaction time of 3 days. The PXRD patterns were recorded after washing the reaction filtrate with acetone and drying the samples in air.

Section 4 Gas Sorption Isotherms for 3D-CageCOF-1

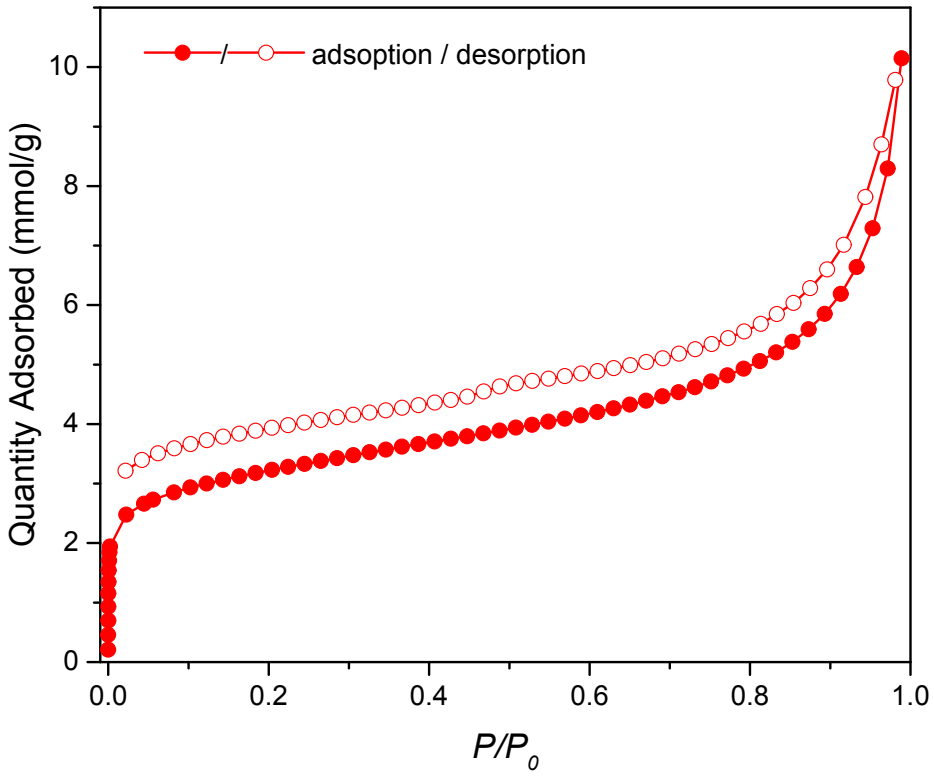

Figure S12 N_2 sorption isotherm recorded at 77 K for a **3D-CageCOF-1** sample that was synthesized without the modulator, aniline, using the following reaction conditions: solvent mixture (NMP: 0.7 mL, MES: 0.3 mL), 6M HOAc (0.1 mL), reaction temperature = 120 °C, and reaction time = 3 days.

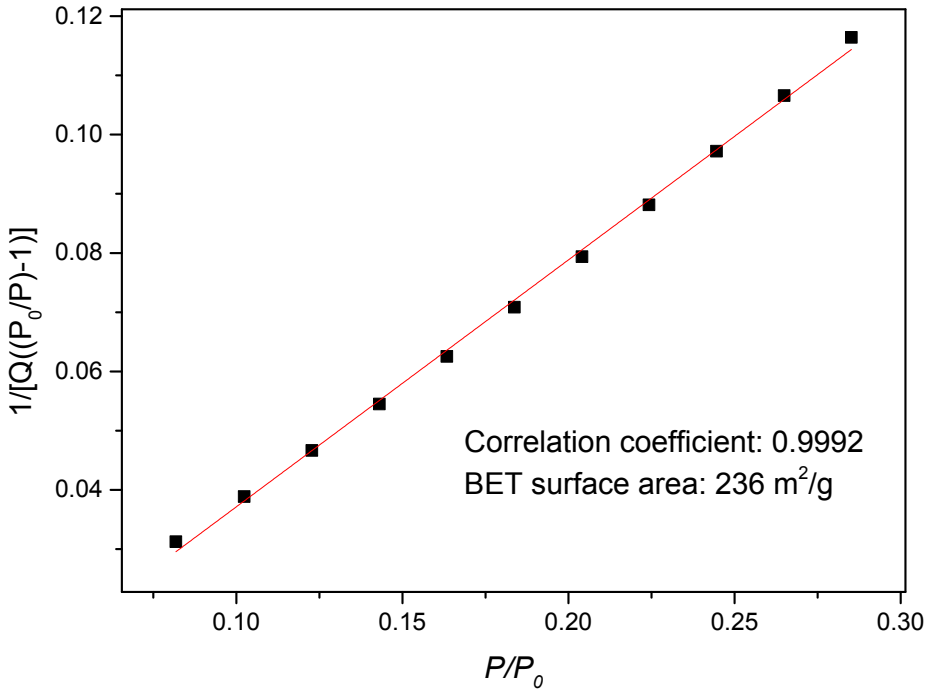

Figure S13 BET surface area plot of **3D-CageCOF-1** that was synthesized without the modulator, aniline.

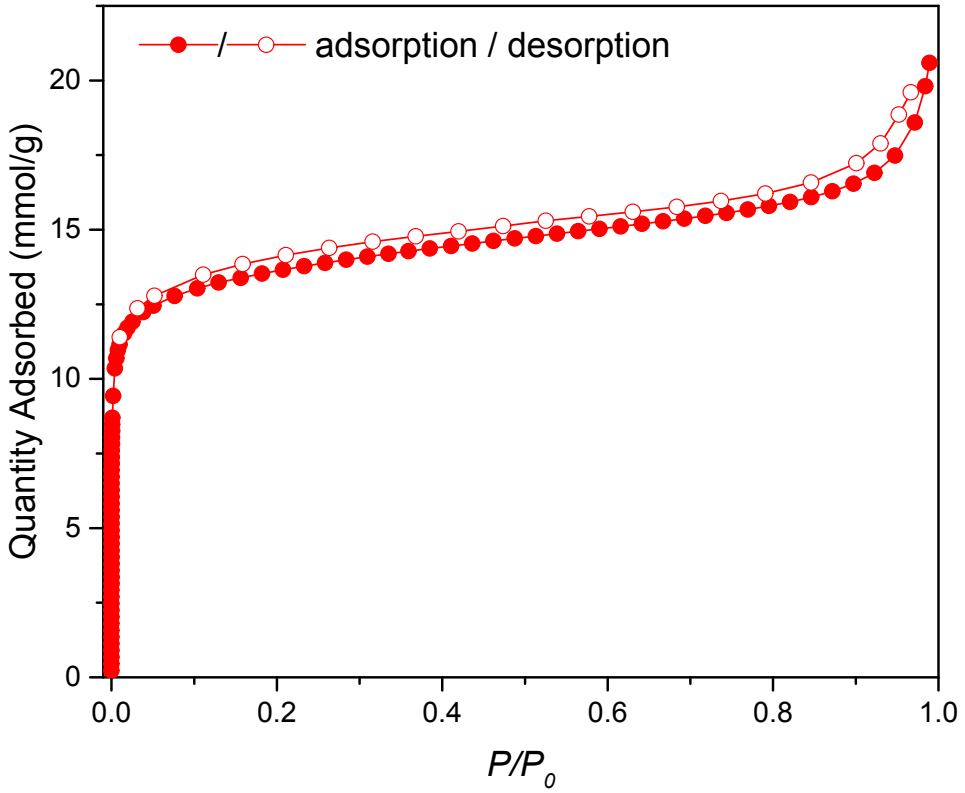

Figure S14 N_2 sorption isotherm recorded at 77 K for **3D-CageCOF-1** sample that was synthesized using the following optimized reaction conditions: 1,4-dioxane (1.0 mL), 6M HOAc (0.1 mL), aniline (20.5 uL), reaction temperature = 120 °C, and reaction time = 3 days.

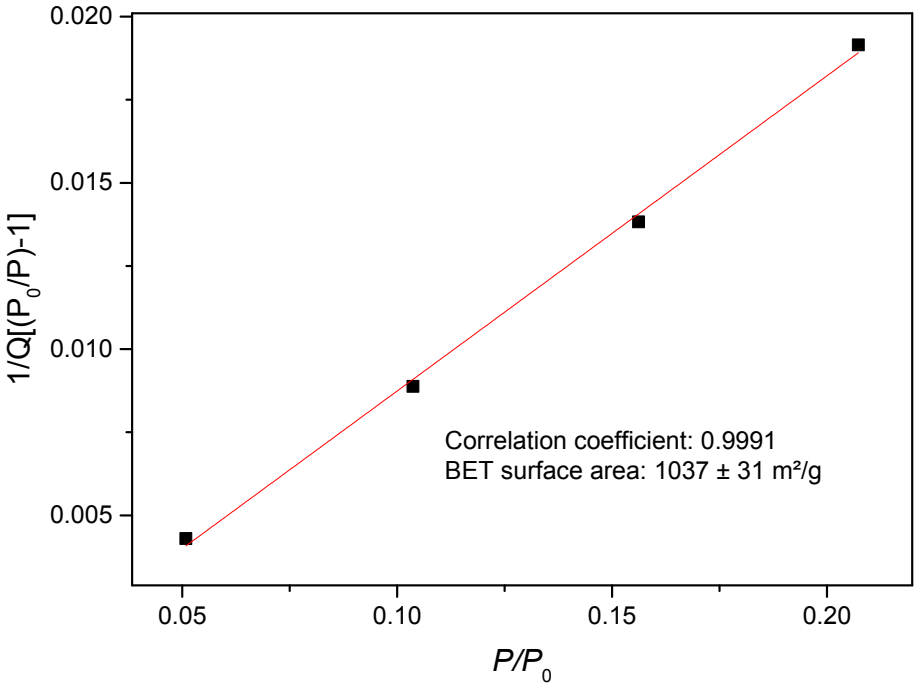

Figure S15 BET surface area plot for **3D-CageCOF-1** sample that was synthesized using the following optimized reaction conditions: 1,4-dioxane (1.0 mL), 6M HOAc (0.1 mL), aniline (20.5 uL), reaction temperature = 120 °C, and reaction time = 3 days.

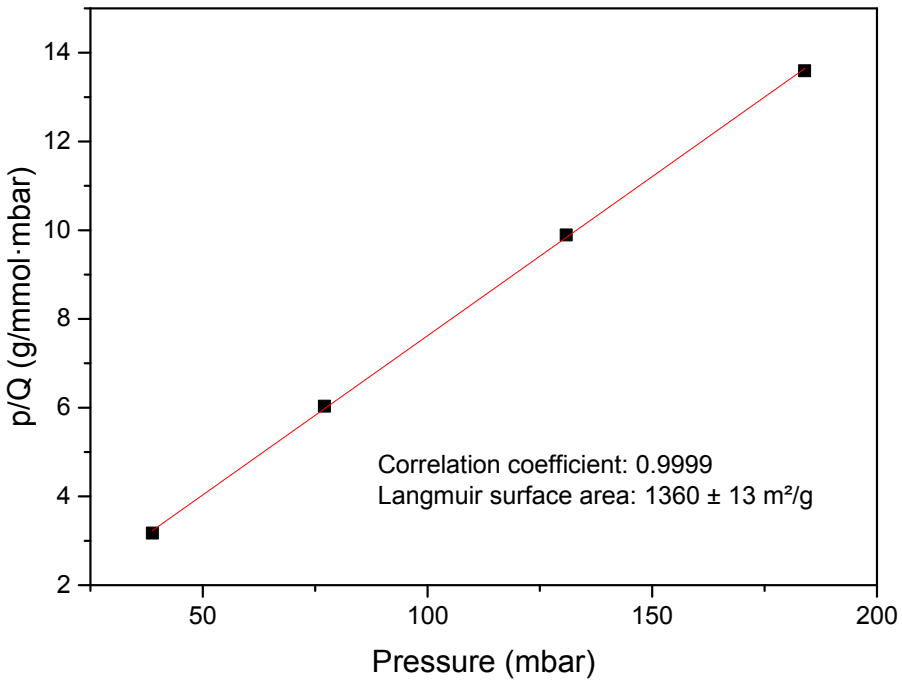

Figure S16 Langmuir surface area plot for **3D-CageCOF-1** sample that was synthesized using the following optimized reaction conditions: 1,4-dioxane (1.0 mL), 6M HOAc (0.1 mL), aniline (20.5 uL), reaction temperature = 120 °C, and reaction time = 3 days.

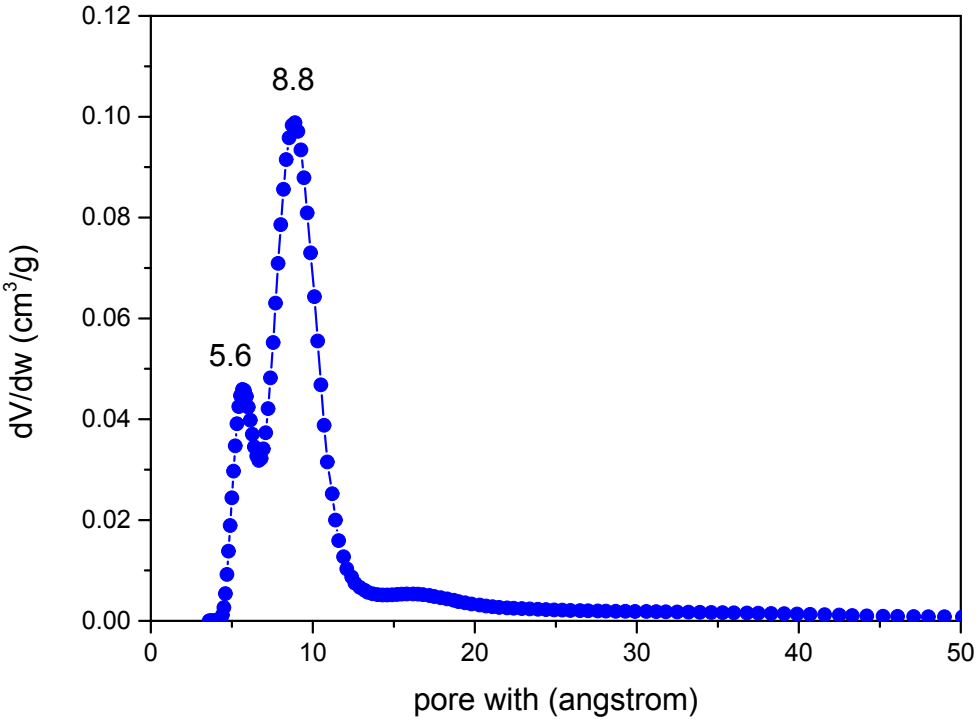

Figure S17 Pore size distribution for **3D-CageCOF-1** sample that was synthesized using the following optimized reaction conditions: 1,4-dioxane (1.0 mL), 6M HOAc (0.1 mL), aniline (20.5 uL), reaction temperature = 120 °C, and reaction time = 3 days. The pore size distribution plot was calculated using the 2D-NLDFT-HS model.[6]

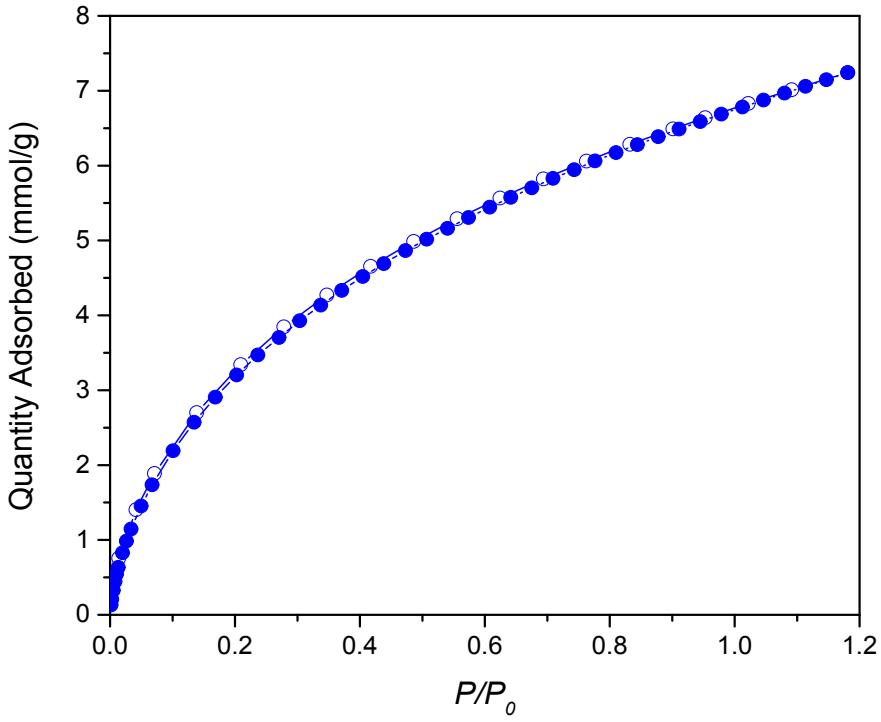

Figure S18 Hydrogen sorption isotherm recorded at 77 K for **3D-CageCOF-1** sample that was synthesized using the following optimized reaction conditions: 1,4-dioxane (1.0 mL), 6M HOAc (0.1 mL), aniline (20.5 uL), reaction temperature = 120 °C, and reaction time = 3 days.

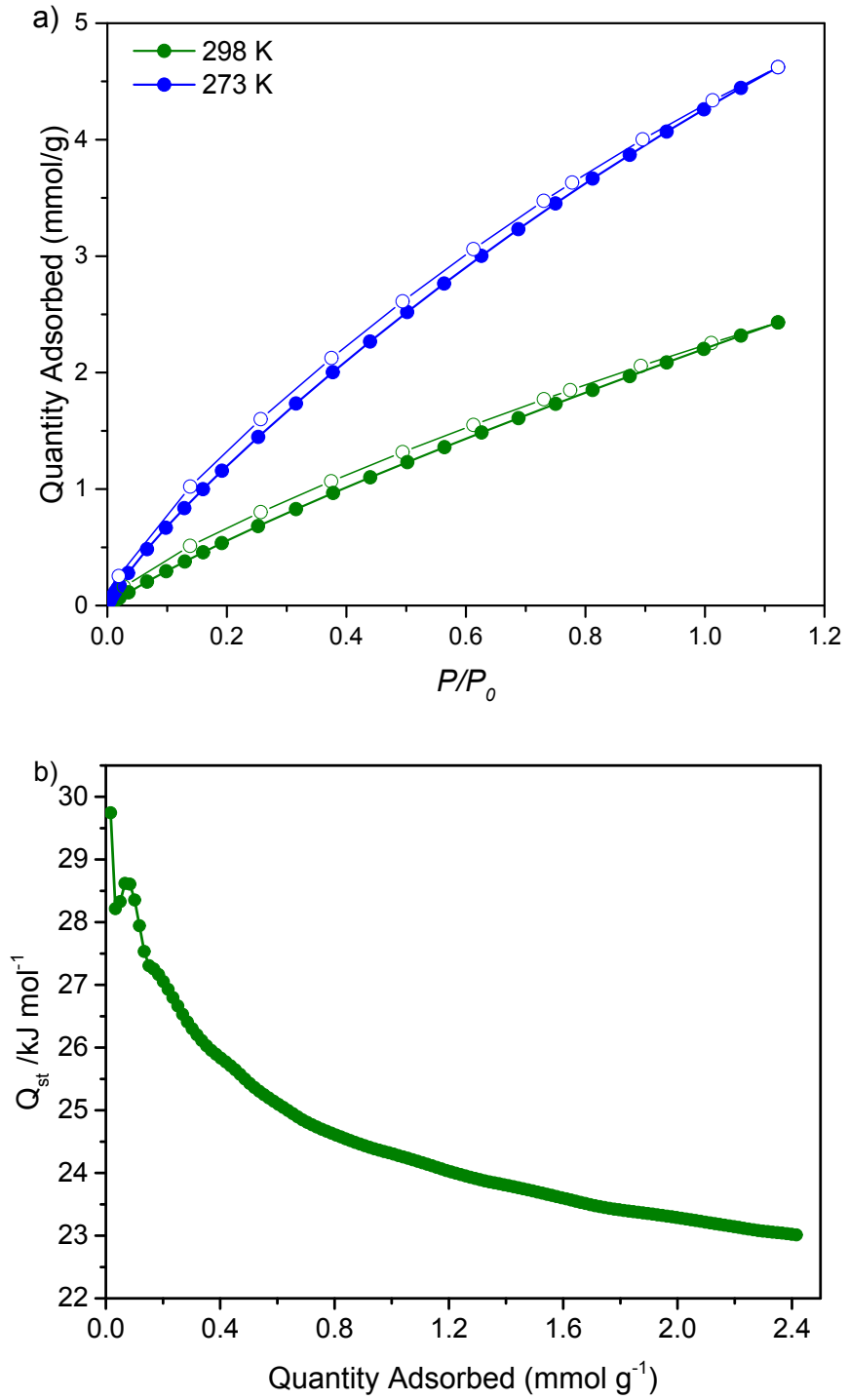

Figure S19 a) CO_2 sorption isotherms recorded at 273 K and 298 K for a **3D-CageCOF-1** sample that was synthesized using the following optimized reaction conditions: solvent = 1,4-dioxane (1.0 mL), 6M HOAc (0.1 mL), aniline (20.5 uL); reaction temperature = 120 °C; and reaction time = 3 days. b) Isosteric heats of adsorption (Q_{st}) for CO_2, calculated using the Clausius–Clapeyron equation and the CO_2 adsorption isotherms in (a).

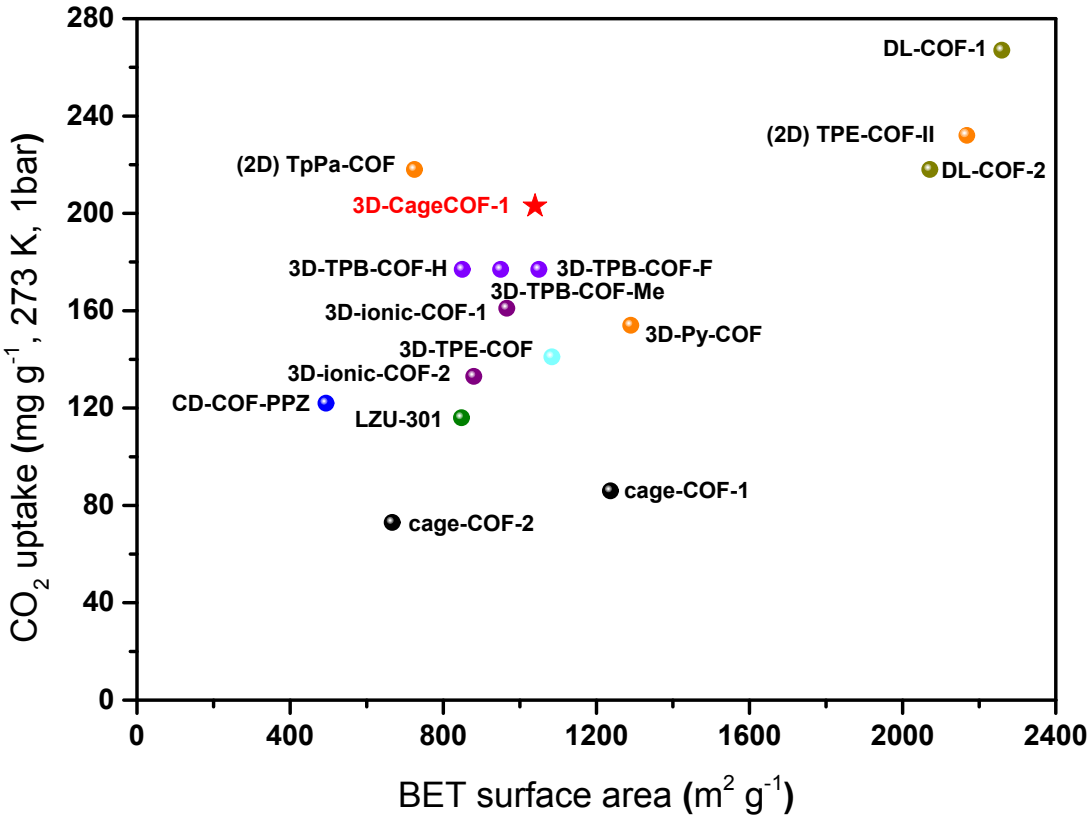

Figure S20 Summary of CO_2 uptake capacities of 3D COFs and 2D cage-COFs at 273 K and 1 bar. **3D-CageCOF-1** is among the top class of COFs for CO_2 uptake. 3D-TPB-COF-H, 3D-TPB-COF-F, 3D-TPB-COF-Me;[7] 3D-ionoc-COF-1, 3D-ionoc-COF-2;[8] 3D-TPE-COF;[9] CD-COF-PPZ;[10] LZU-301;[11] 3D-Py-COF;[12] DL-COF-1, DL-COF-2;[13] cage-COF-1, cage-COF-2;[14] TpPa-COF;[15] TPE-COF-II[16, 17].

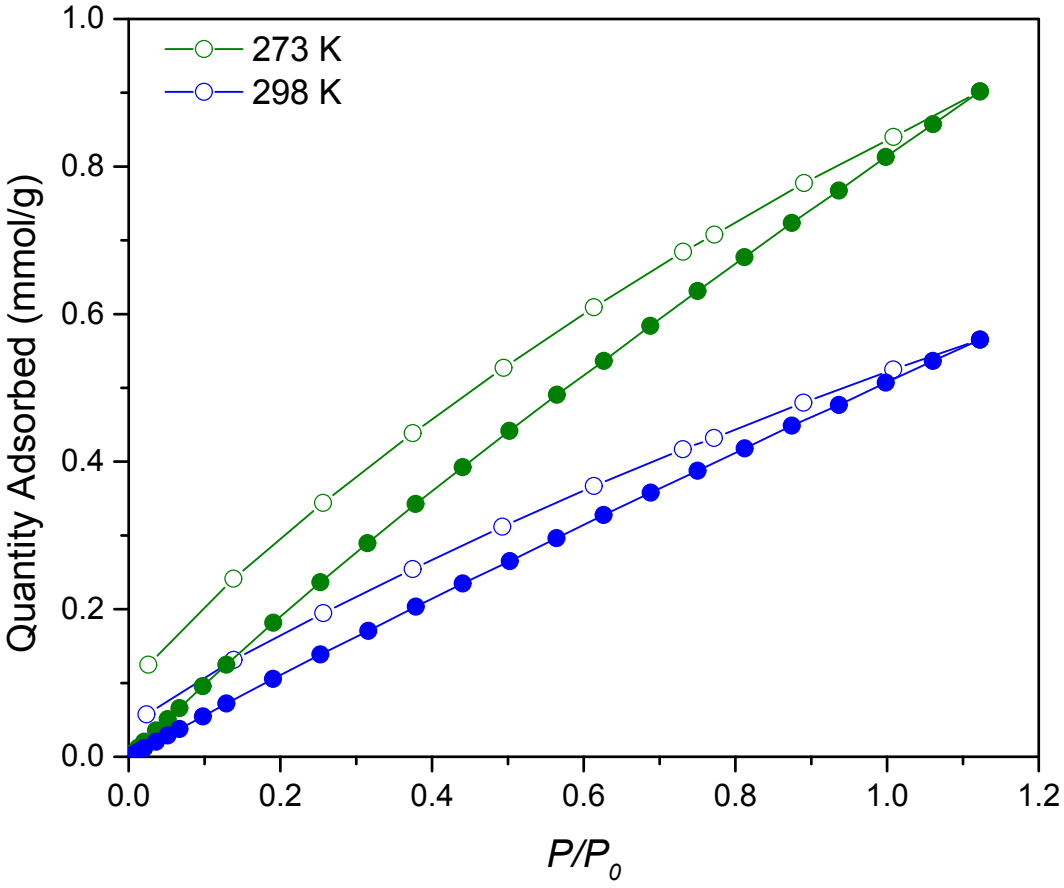

Figure S21 CH_4 sorption isotherms at 273 K and 298 K for a **3D-CageCOF-1** sample that was synthesized using the following optimized reaction conditions: 1,4-dioxane (1.0 mL), 6M HOAc (0.1 mL), aniline (20.5 uL), reaction temperature = 120 °C, and reaction time = 3 days.

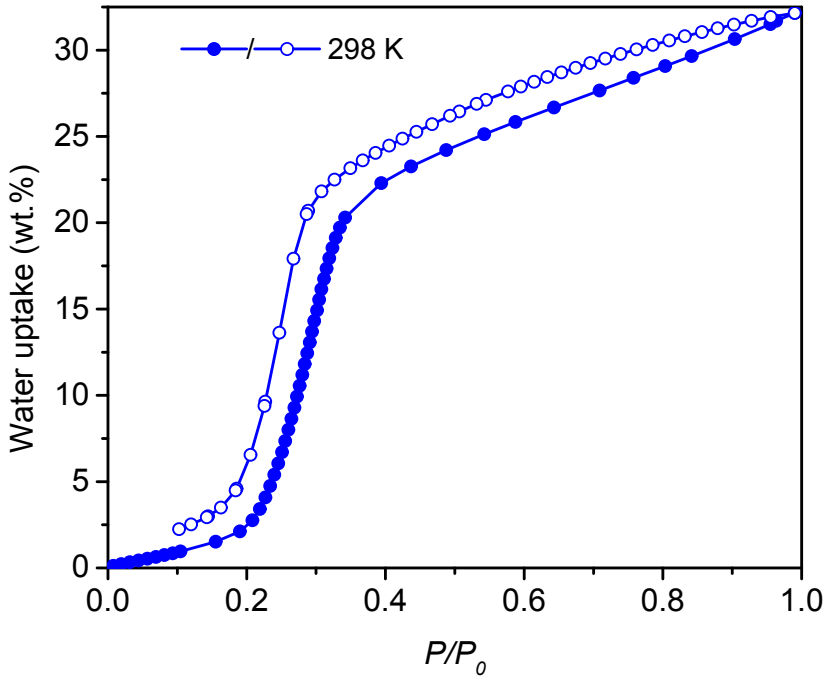

Figure S22 Water vapor sorption isotherms at 298 K for a **3D-CageCOF-1** sample that was synthesized using the following optimized reaction conditions: 1,4-dioxane (1.0 mL), 6M HOAc (0.1 mL), aniline (20.5 uL), reaction temperature = 120 °C, and reaction time = 3 days.

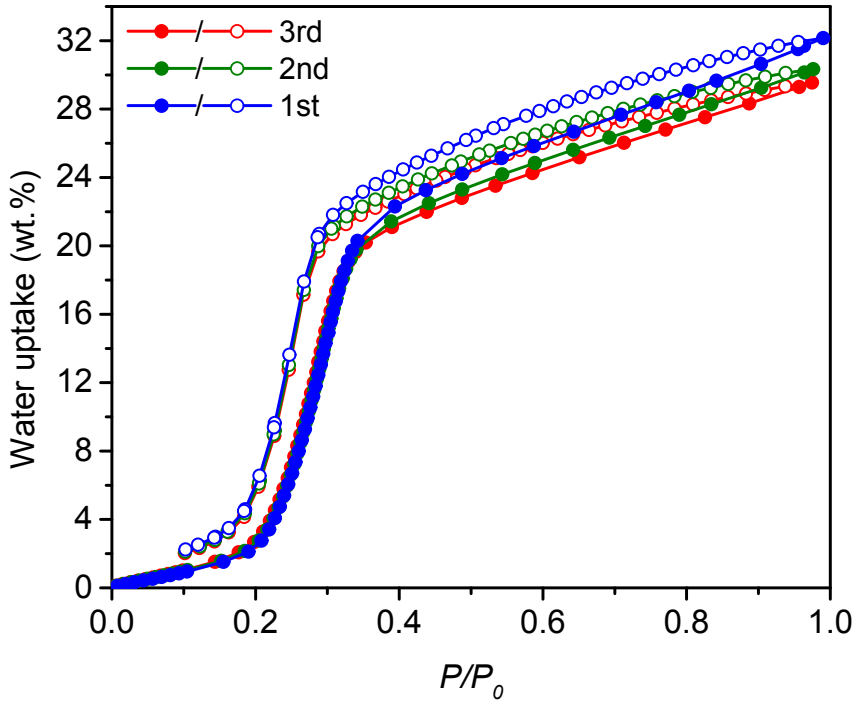

Figure S23 Recycle performance of **3D-CageCOF-1** for water vapor sorption isotherms recorded at 298 K. **3D-CageCOF-1** sample that was synthesized using the following optimized reaction conditions: 1,4-dioxane (1.0 mL), 6M HOAc (0.1 mL), aniline (20.5 uL), reaction temperature = 120 °C, and reaction time = 3 days.

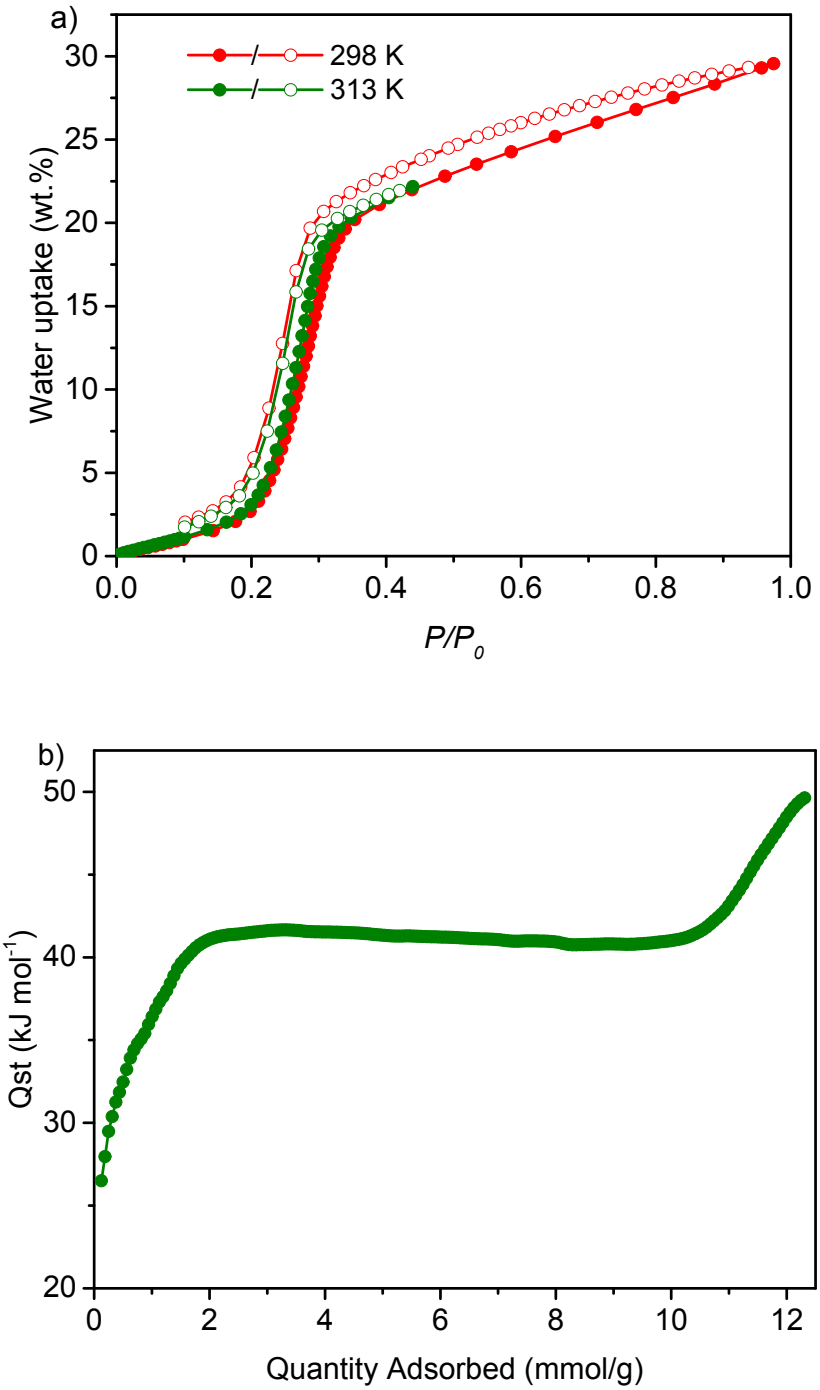

Figure S24 a) Comparison of water vapor sorption isotherms for the optimized **3D-CageCOF-1** sample at 298 K and 313 K. The plot indicates that **3D-CageCOF-1** exhibits high water uptake at low relative pressure, even when the temperature is increased to 313 K. At 313 K, measurements up to the relative pressure of 0.5 could only be recorded due to limitations associated with the instrumentation. b) Isosteric heats of adsorption (Q_{st}) for H_2O, calculated using the Clausius–Clapeyron equation and the H_2O adsorption isotherms in (a).

Section 5 Structural Modelling for 3D-CageCOF-1

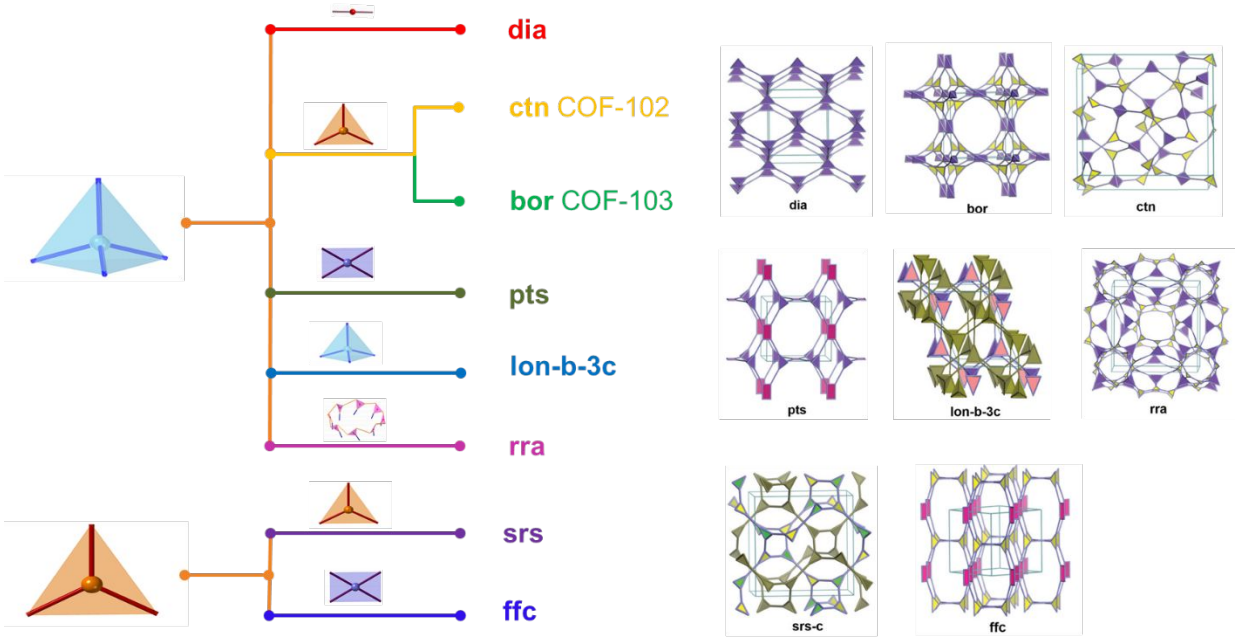

Figure S25 Topologies reported for 3D COFs.[18]

Table S2. Topological preference ranking for **3D-CageCOF-1** by mean average angle deviation (AAD)[a].

topology	**acs**	**snx**	**snw**	**lcy**
no. of edges	1	2	2	1
mean AAD (°)	0.35	1.22	1.58	4.32

[a.] The AAD is a measure of how well the chosen building blocks fit on a target crystal net; the smaller the AAD value, the better the fit of the building blocks to the target topology. For each topology, the mean AAD value reported above corresponds to the most optimized embedding orientation of the building blocks into the net. Here, we used maximum symmetry embedded topologies as blueprints without further optimization, and the cage building block adopted a highly symmetrical, trigonal prism geometry. The AAD analyses were carried out using the weaver code developed by Schmid and co-workers.[19] According to the AAD results, **acs** is the most preferred topology for the organic cage building block.

Table S3. Unit cell parameters and porosity characteristics of the simulated models for **3D-CageCOF-1**. [a]

	small-pore					large-pore				
	space group	a=b (Å)	c (Å)	D_i, D_f [d] (Å)	ASA [e] (m^2 g^{-1})	space group	a=b (Å)	c (Å)	D_i, D_f (Å)	ASA (m^2 g^{-1})
onefold [b]	n/a	n/a	n/a	n/a	n/a	P63/M	24.0	23.9	19.1, 17.8	5930.4
twofold [c]	P-3	19.4	24.5	8.5, 5.1	1923.5	P-3	25.5	22.9	11.8, 9.1	4125.5
threefold [c]	P63	18.9	24.9	6.4, 2.4	0	P63	25.5	22.9	6.8, 4.6	2008.1

[a] All structures were optimized by periodic DFT calculations within the plane-wave pseudopotential formalism, using the Vienna ab initio Simulation Package (VASP) code. Geometry optimizations were performed with the Perdew–Burke–Ernzerhof exchange–correlation functional with the DFT-D3(BJ) dispersion correction. A kinetic-energy cutoff of 500 eV was used to define the plane-wave basis set. All porosity parameters were calculated using zeo++.

[b] For the non-interpenetrated (onefold) form, the large-pore structure is stable and was optimized to the cell parameters as reported in the table. Therefore, there is no small-pore structure for it.

[c] For the twofold and threefold interpenetrations, the large-pore structure is not stable and was optimized to a small-pore structure, with the cell parameters shown in the table. The large-pore structures shown here for the twofold and threefold forms were optimized with the cell parameters fixed at the experimental values.

[d] D_i: diameter of the largest included sphere; D_f: diameter of the largest free sphere.

[e] ASA: accessible surface area, determined by a probe radius of 1.82 Å (half of N_2 molecule's kinetic diameter).

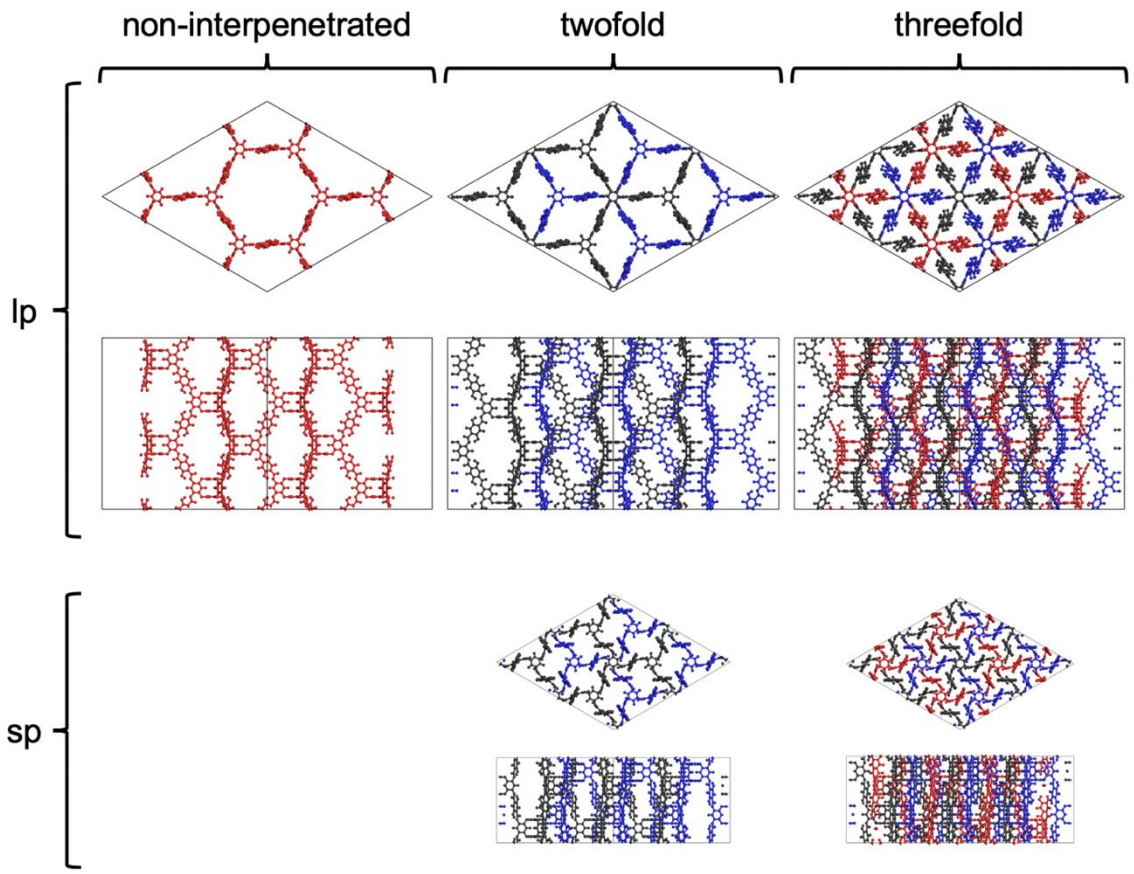

Figure S26. Structural models simulated for **3D-CageCOF-1**: **lp**, large-pore; **sp**, small-pore.

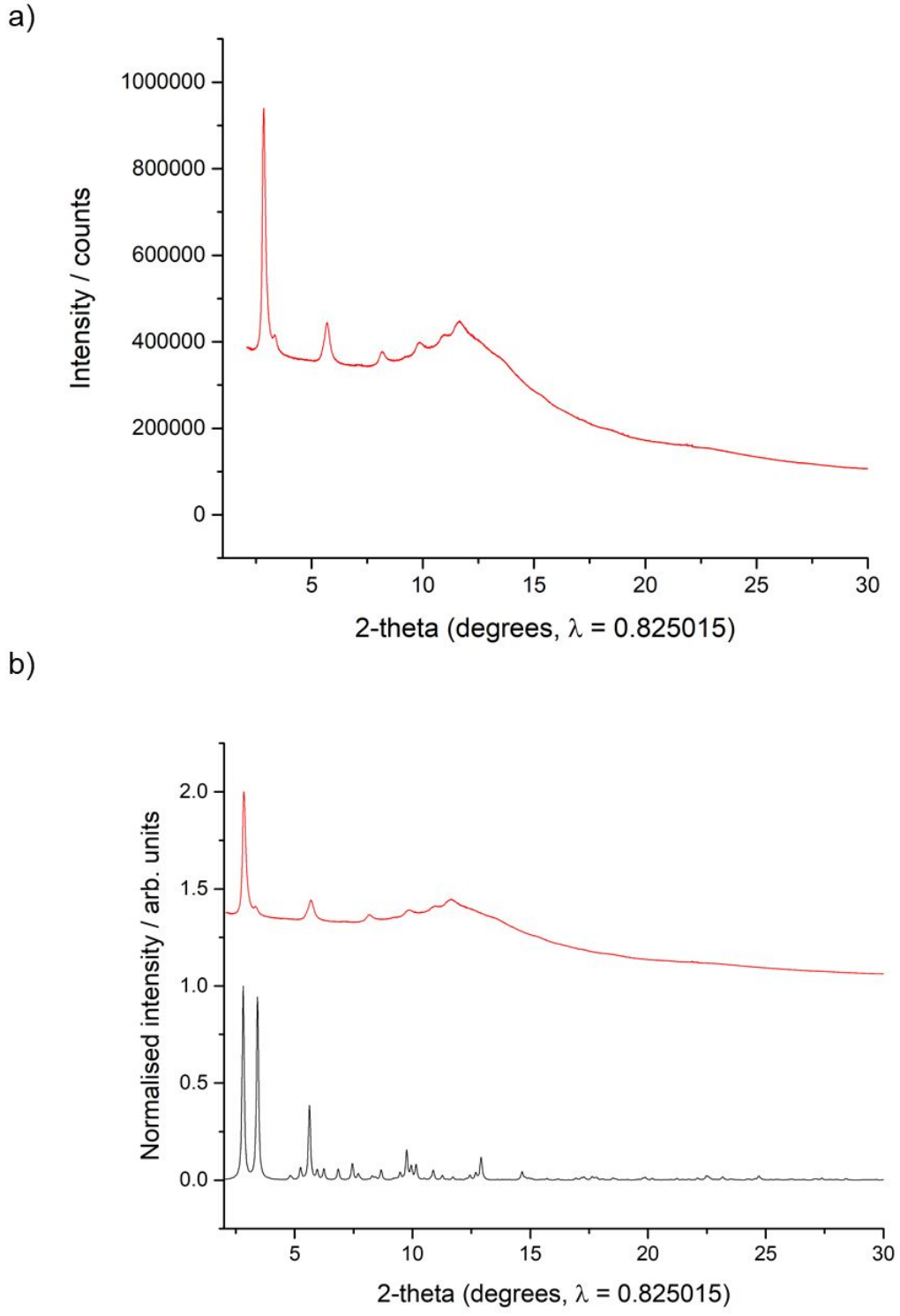

Figure S27 a) PXRD pattern for activated **3D-CageCOF-1** that was collected using synchrotron radiation (λ = 0.825015). Refining the broad peaks at 2.82° (d-spacing (Å) = 16.746) and 5.65° (d-spacing (Å) = 8.373) in the diffraction pattern as the [100] and [200] reflections, respectively, for a trigonal/hexagonal structure, correspond to a *a*=*b* unit cell edge of ~19.4 Å unit cell edge. b) Comparison between the experimental PXRD pattern of activated **3D-CageCOF-1** (top, red) collected using synchrotron radiation (λ = 0.825015) and the simulated PXRD for the **sp** model of **3D-CageCOF-1** (bottom, black).

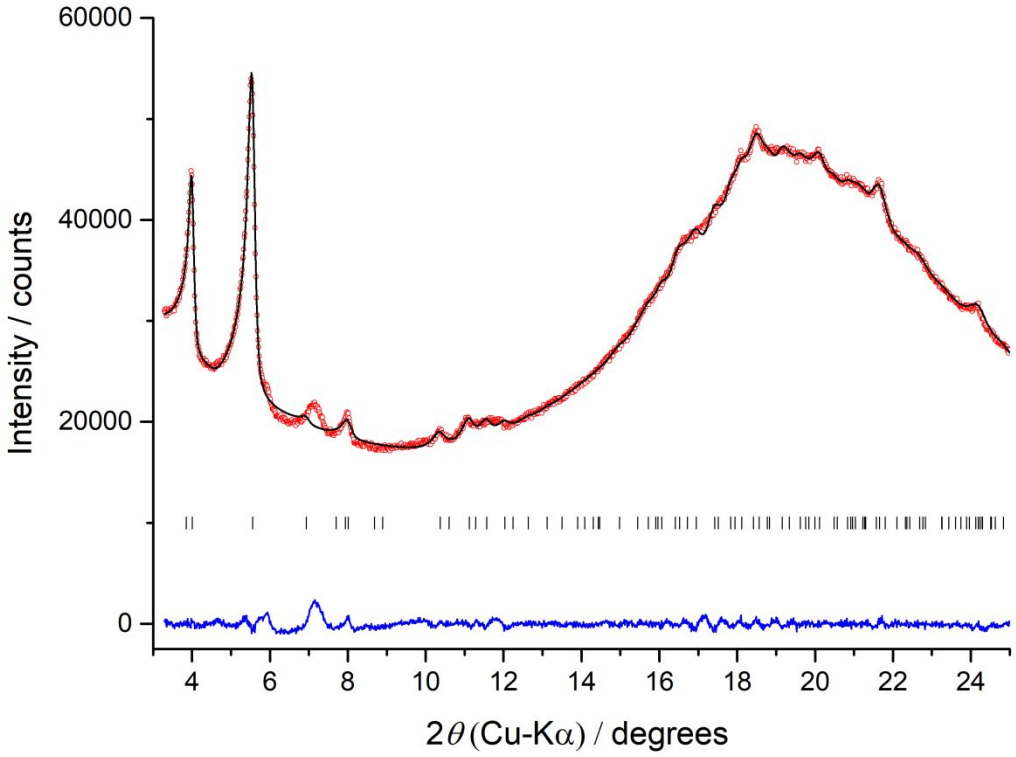

Figure S28 PXRD pattern fitting of **3D-CageCOF-1**·DMF with Pawley refinement (Cu-Kα). Red circles: experimental PXRD pattern, black line: fitting pattern, blue curve: difference between experimental and refinement, black bars: reflection positions, Rp = 0.8%, Rwp = 1.4%, χ = 2.6% ($P\bar{3}$, $a = b$ = 25.5 Å, c = 22.9 Å, V = 12880 Å^3).

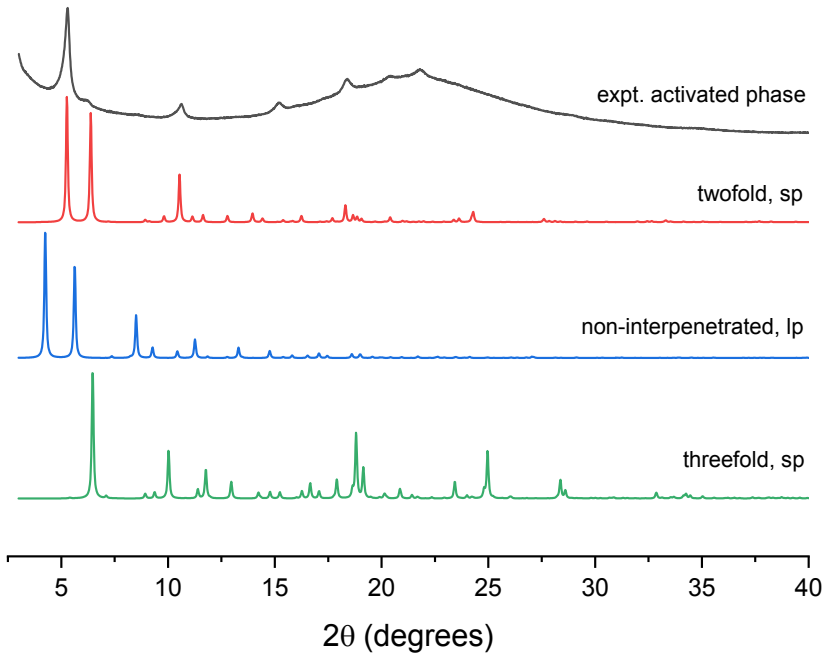

Figure S29 Comparison of PXRD patterns between the experimental activated phase and the atomistic models.

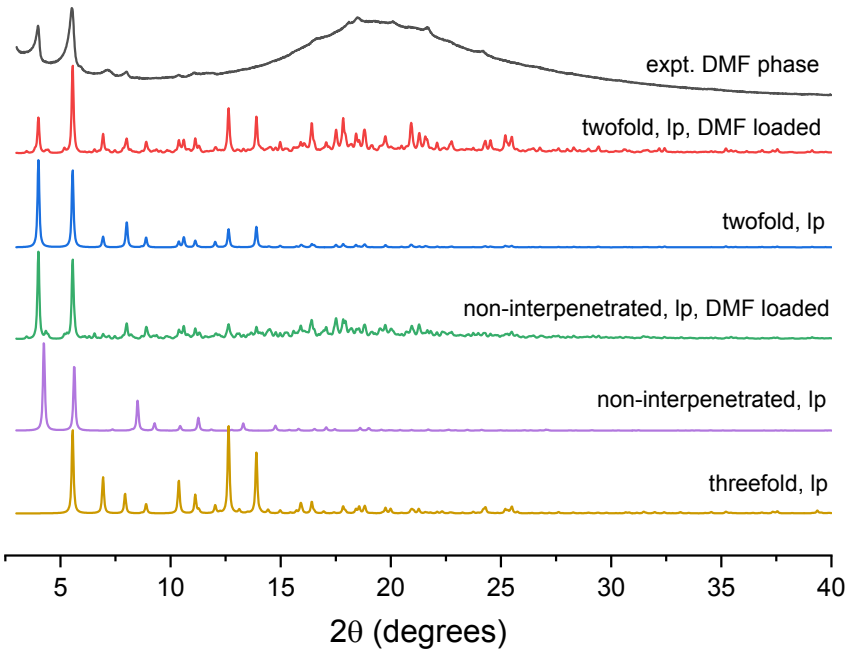

Figure S30 Comparison of PXRD patterns between the experimental DMF phase and the atomistic models.

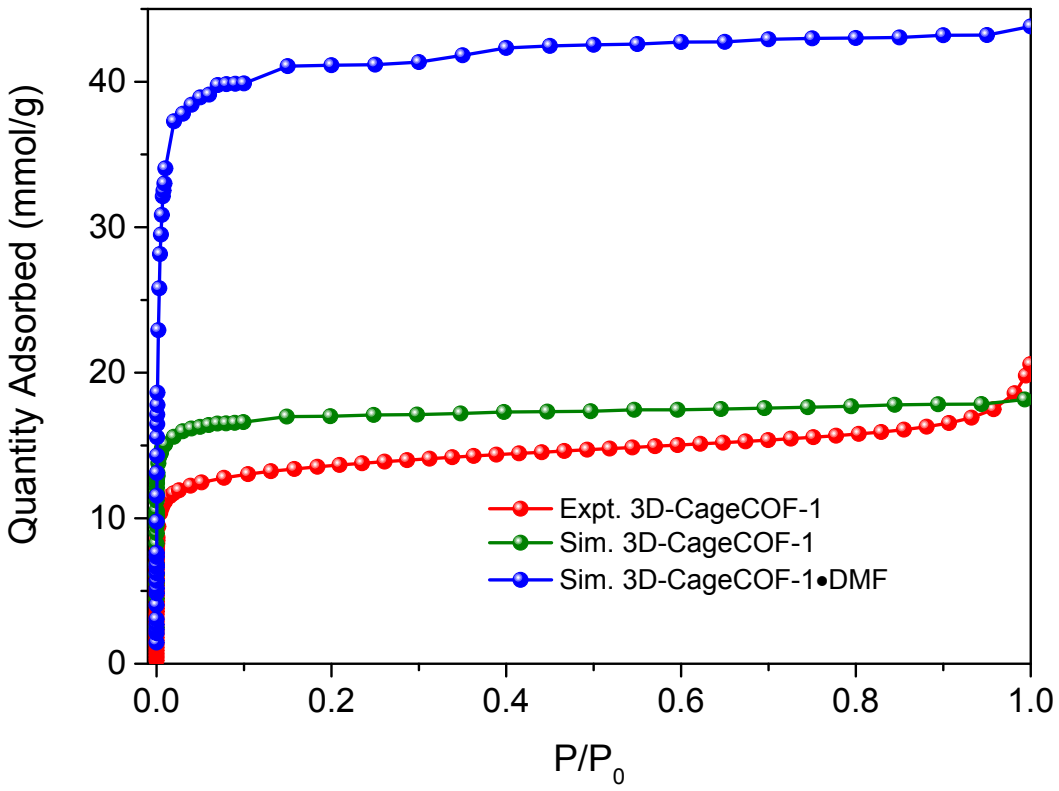

Figure S31 Experimental and simulated N_2 adsorption isotherms of **3D-CageCOF-1** and **3D-CageCOF-1**·DMF, at 77 K.

Section 6 Scanning Electronic Microscopy and Transmission Electron Microscopy Images for 3D-CageCOF-1

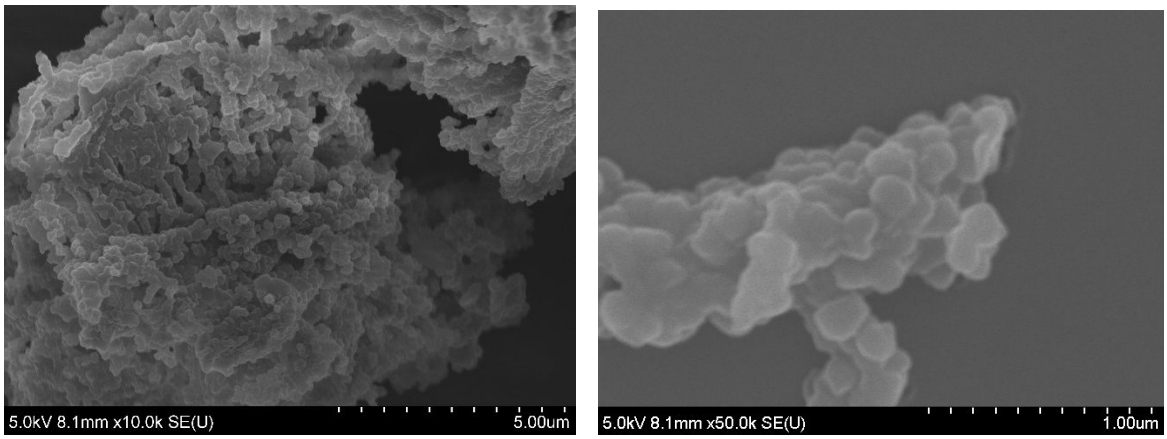

Figure S32 SEM images of activated **3D-CageCOF-1** sample that was synthesized using the following optimized reaction conditions: 1,4-dioxane (1.0 mL), 6M HOAc (0.1 mL), aniline (20.5 uL), reaction temperature = 120 °C, and reaction time = 3 days.

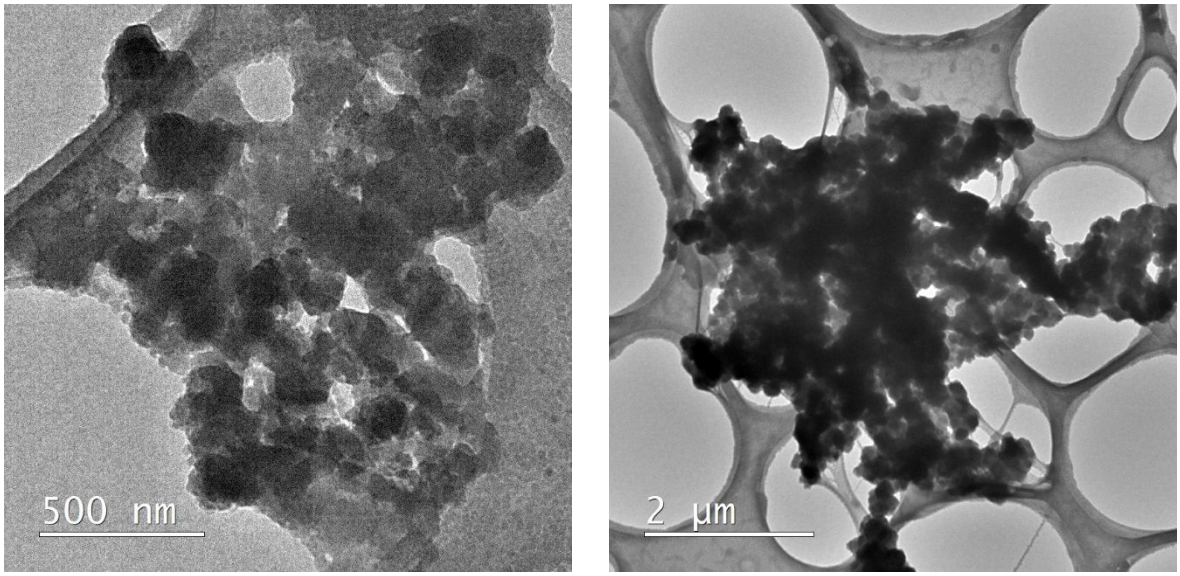

(A) (B)

Figure S33 TEM images of activated **3D-CageCOF-1** sample that was synthesized using the following optimized reaction conditions: 1,4-dioxane (1.0 mL), 6M HOAc (0.1 mL), aniline (20.5 uL), reaction temperature = 120 °C, and reaction time = 3 days.

Section 7 Fourier-transform Infrared Spectra and Solid-State NMR Spectrum for 3D-CageCOF-1

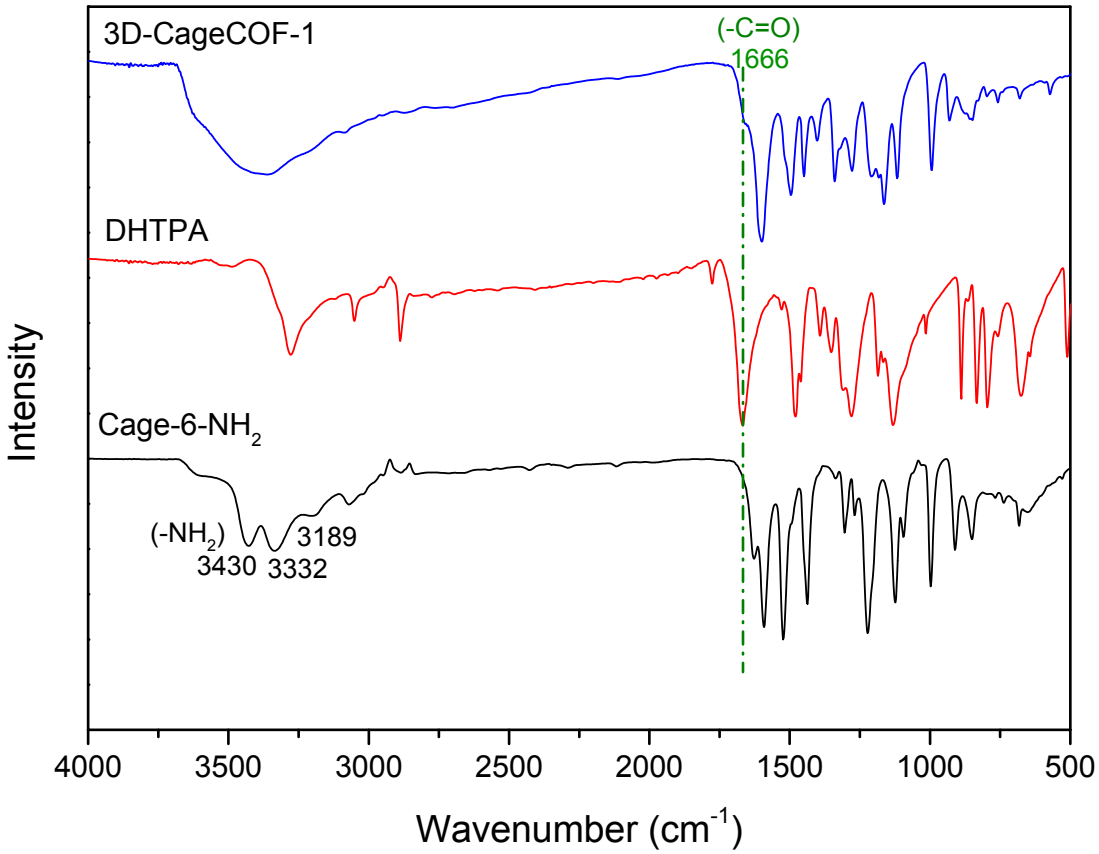

Figure S34 FT-IT spectrum of activated **3D-CageCOF-1** sample that was synthesized using the following optimized reaction conditions: 1,4-dioxane (1.0 mL), 6M HOAc (0.1 mL), aniline (20.5 uL), reaction temperature = 120 °C, and reaction time = 3 days.

.

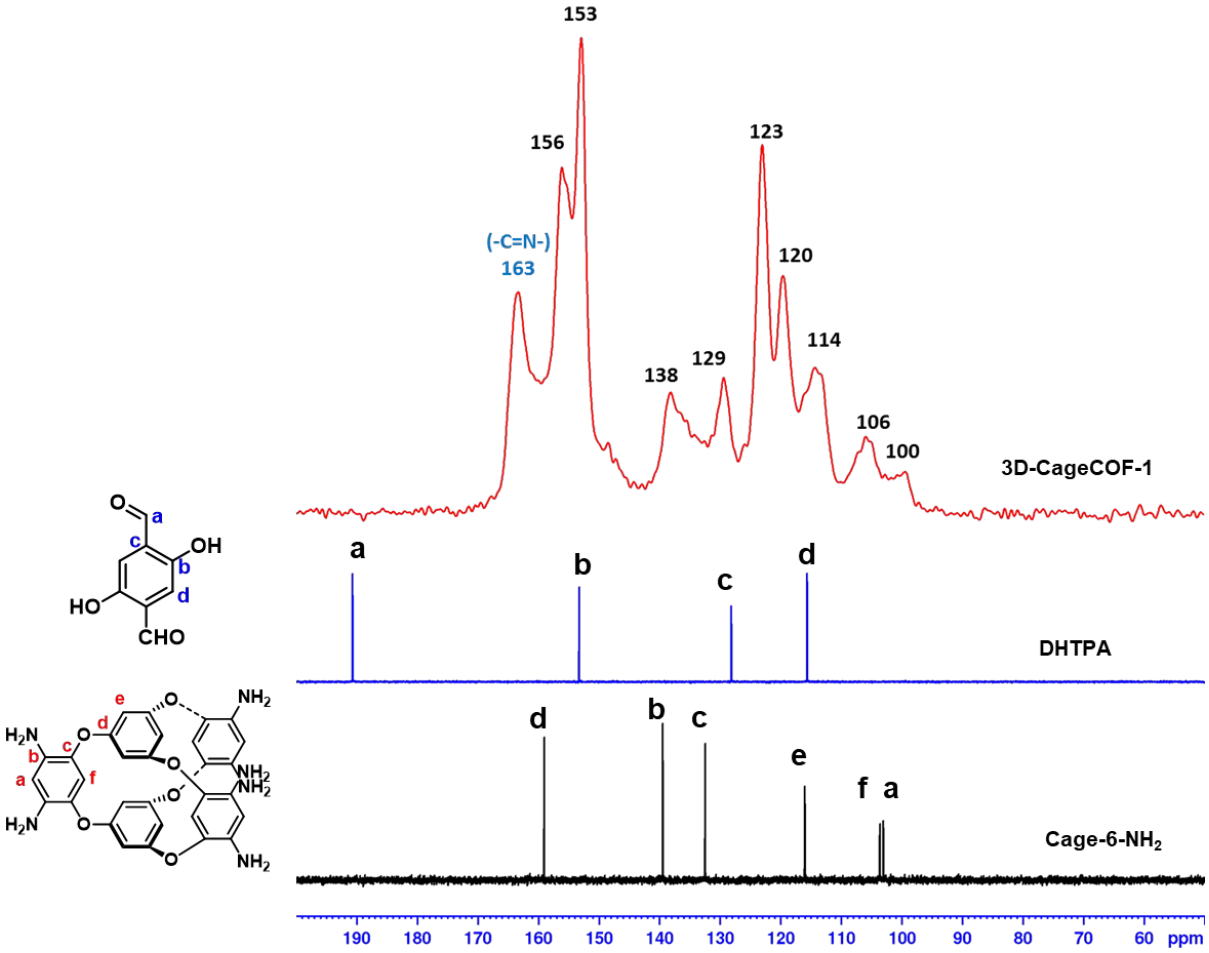

Figure S35 ^{13}C solid state NMR CP/MAS spectrum of activated **3D-CageCOF-1** sample that was synthesized using the following optimized reaction conditions: 1,4-dioxane (1.0 mL), 6M HOAc (0.1 mL), aniline (20.5 uL), reaction temperature = 120 °C, and reaction time = 3 days.

Section 8 Thermogravimetric Analysis and Solid-state UV-vis Spectra for 3D-CageCOF-1

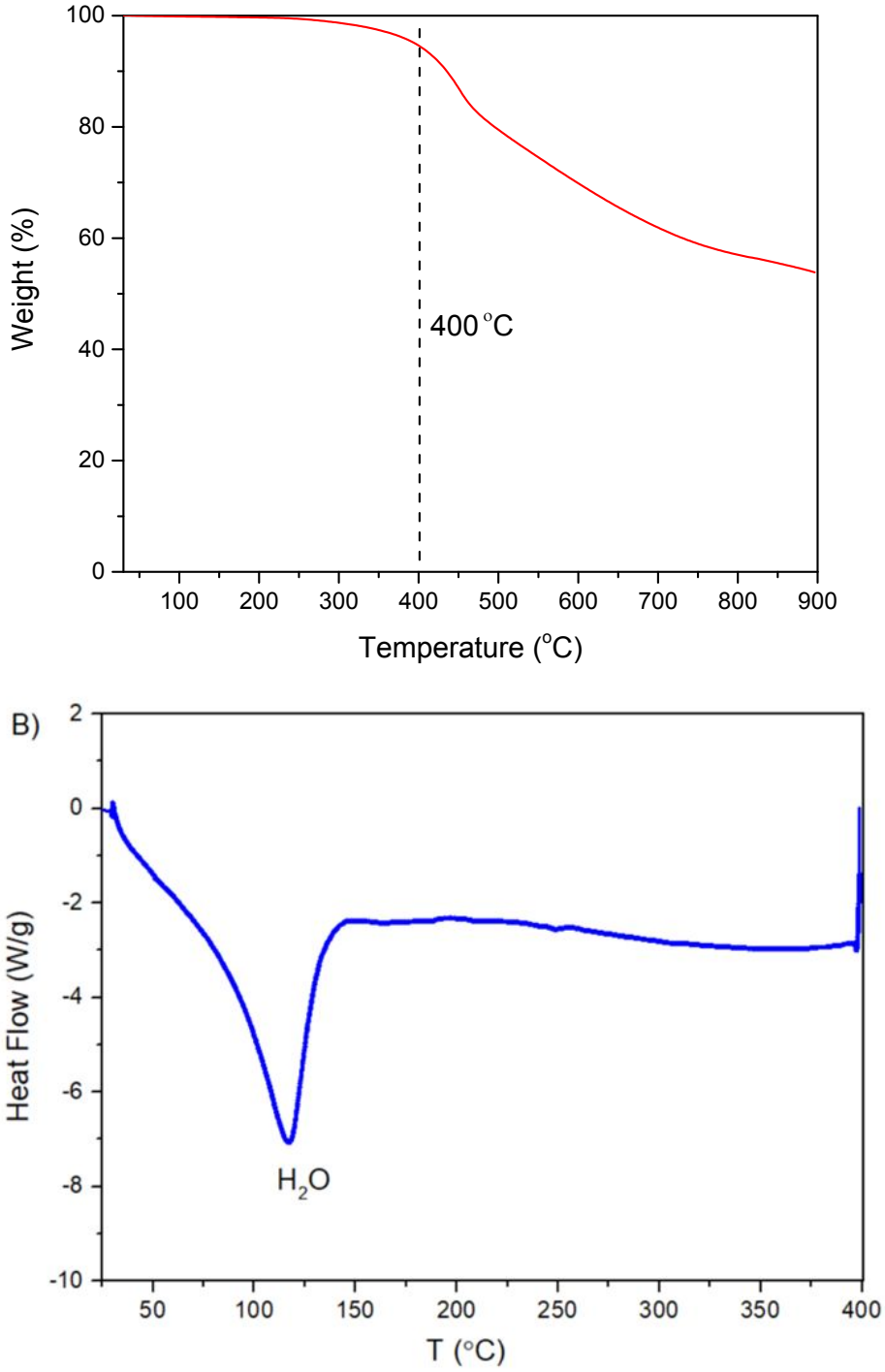

Figure S36. a) TGA plot for a freshly activated sample of **3D-CageCOF-1**, which shows no significant weightloss was recorded up to ~400 °C. b) DSC plot for **3D-CageCOF-1** sample that shows loss of water from the COF at temperatures < 140 °C, but no evidence of any further processes occurring between 140 °C and the onset of weightloss in the TGA plot. The **3D-CageCOF-1** samples were synthesized using the following optimized reaction conditions: 1,4-dioxane (1.0 mL), 6M HOAc (0.1 mL), aniline (20.5 uL), reaction temperature = 120 °C, and reaction time = 3 days.

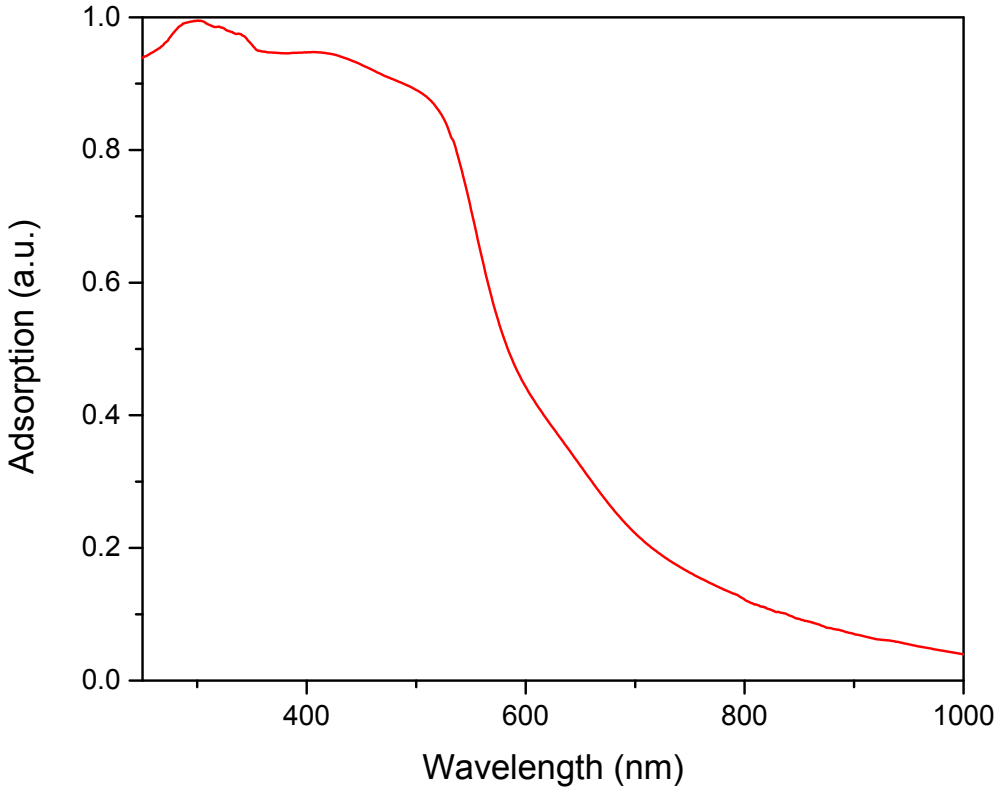

Figure S37 Solid-state UV-vis spectra of an activated **3D-CageCOF-1** sample that was synthesized using the following optimized reaction conditions: 1,4-dioxane (1.0 mL), 6M HOAc (0.1 mL), aniline (20.5 uL), reaction temperature = 120 °C, and reaction time = 3 days.

Section 9 Stability Tests for 3D-CageCOF-1

To determine the stability of **3D-CageCOF-1** that was synthesized using the optimized reaction conditions, powdered samples (~20 mg) were immersed in different organic solvents or aqueous solutions (20 ml) at room temperature for 24 hours. The **3D-CageCOF-1** was isolated by filtration and then washed by Soxhlet extraction with acetone for 4 hours, dried in the air, and then characterized by PXRD and FT-IR. From these experiments, we determined that **3D-CageCOF-1** decomposed in 1 M HCl and 1 M NaOH aqueous solutions. The results from the other solvents are shown in Figure S38:

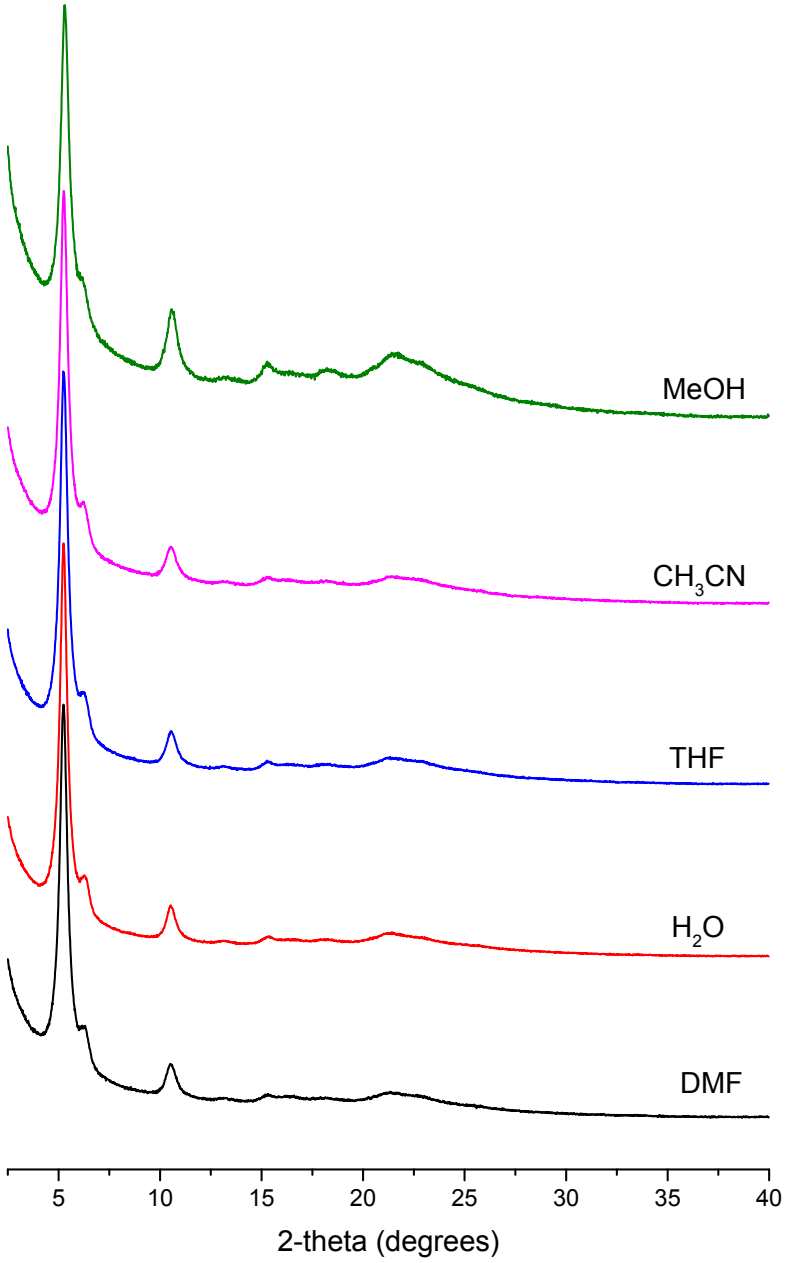

Figure S38 PXRD profiles of activated **3D-CageCOF-1** after treating with various solutions. The powdered samples were synthesized using the following optimized reaction conditions: 1,4-dioxane (1.0 mL), 6M HOAc (0.1 mL), aniline (20.5 uL), reaction temperature = 120 °C, and reaction time = 3 days.

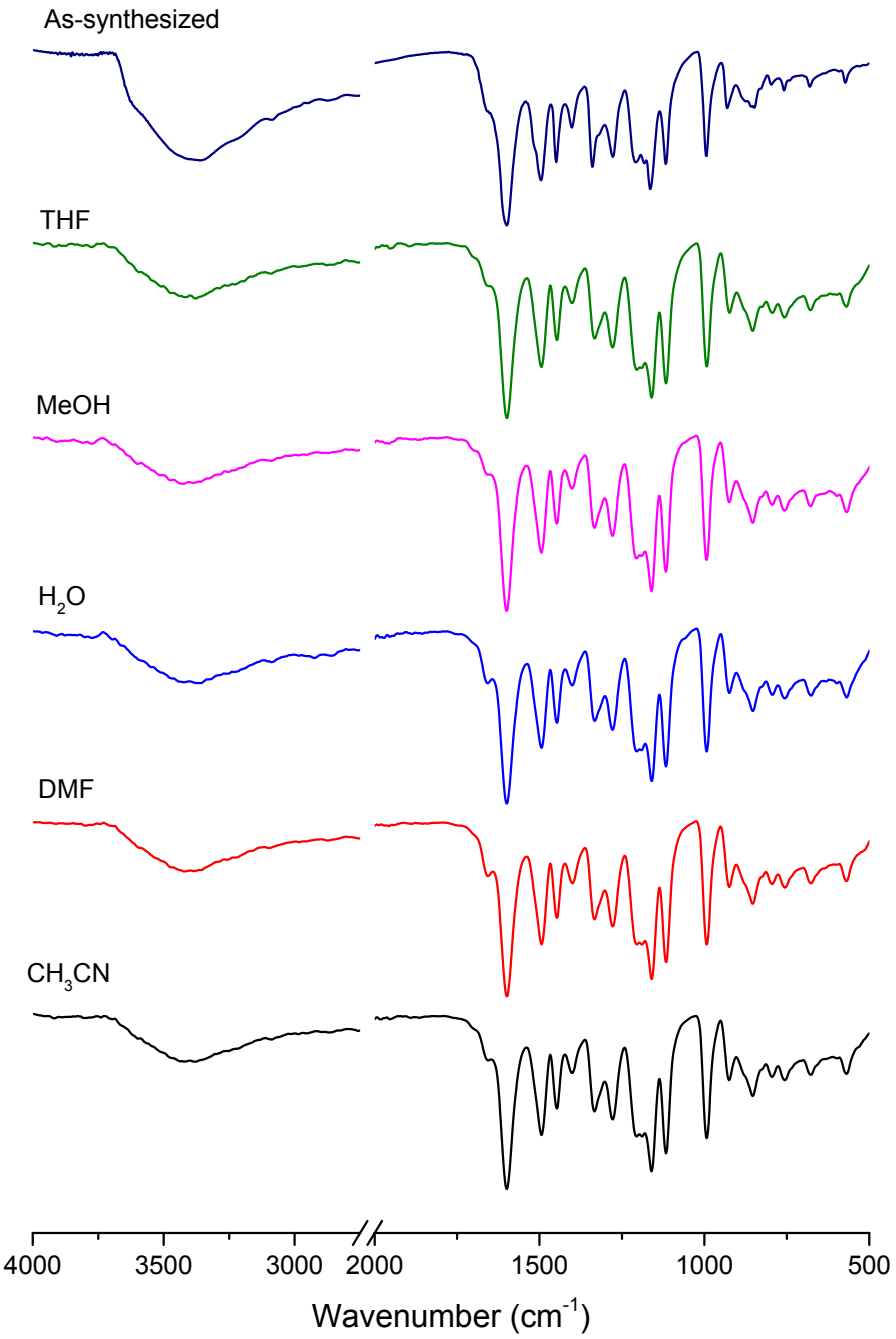

Figure S39 FT-IR profiles of activated **3D-CageCOF-1** after treating with various organic solvent. The powder sample was synthesized using the following optimized reaction conditions: 1,4-dioxane (1.0 mL), 6M HOAc (0.1 mL), aniline (20.5 uL), reaction temperature = 120 °C, and reaction time = 3 days.

Section 10 Characterization of Dynamic Behaviour of 3D-CageCOF-1

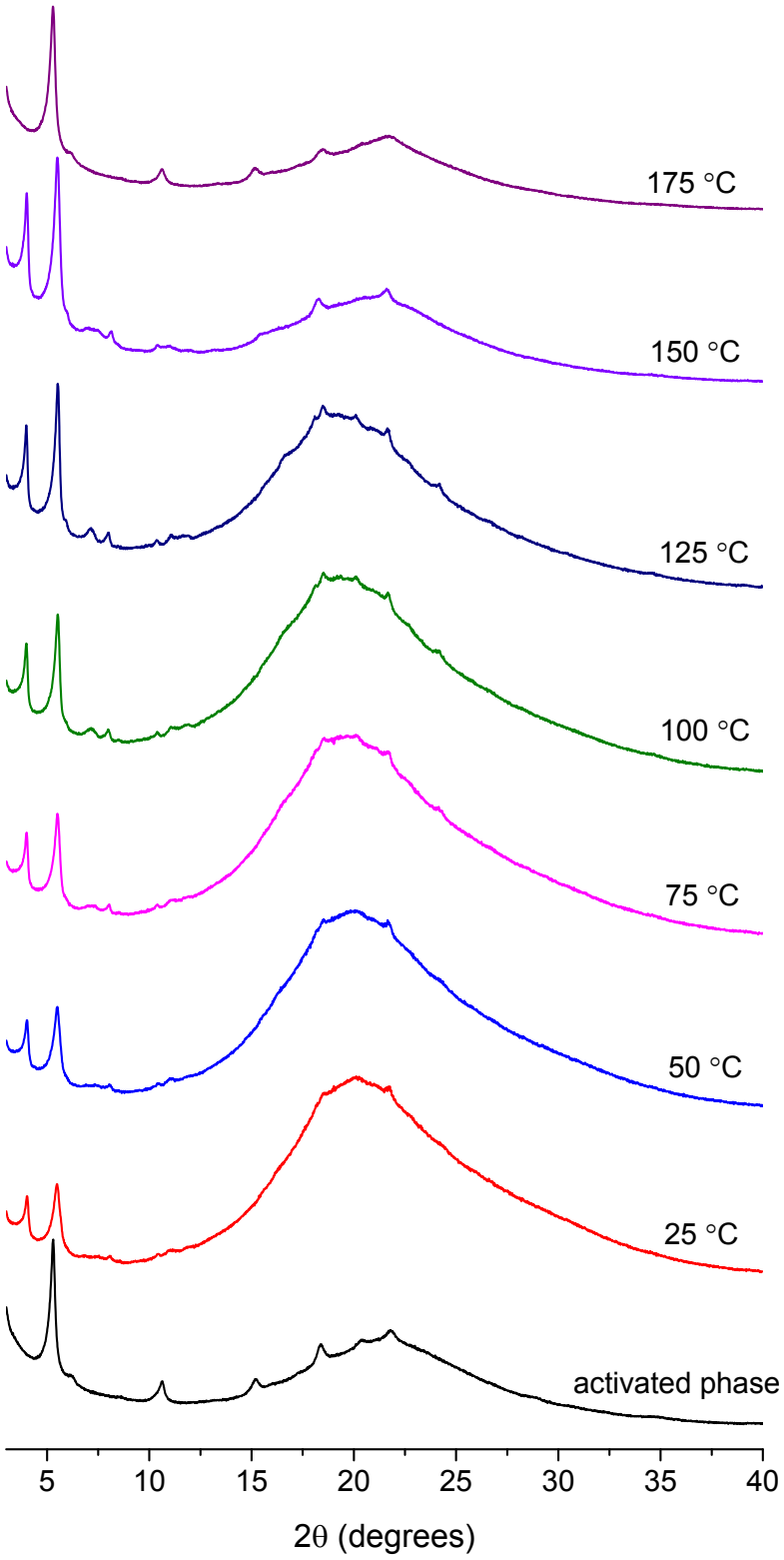

Figure S40. *In situ* PXRD patterns that were recorded after heating a DMF solvated sample of **3D-CageCOF-1** that was synthesized using the optimized reaction condition from 25 °C to 175 °C. The capillary temperature was increased by 25 °C between the measurements and left to equilibrate for 1 hour at each temperature before the PXRD patterns were recorded.

Section 11 Single Crystal X-ray Diffraction Data for Cage-6-NO_2 and Model Compound

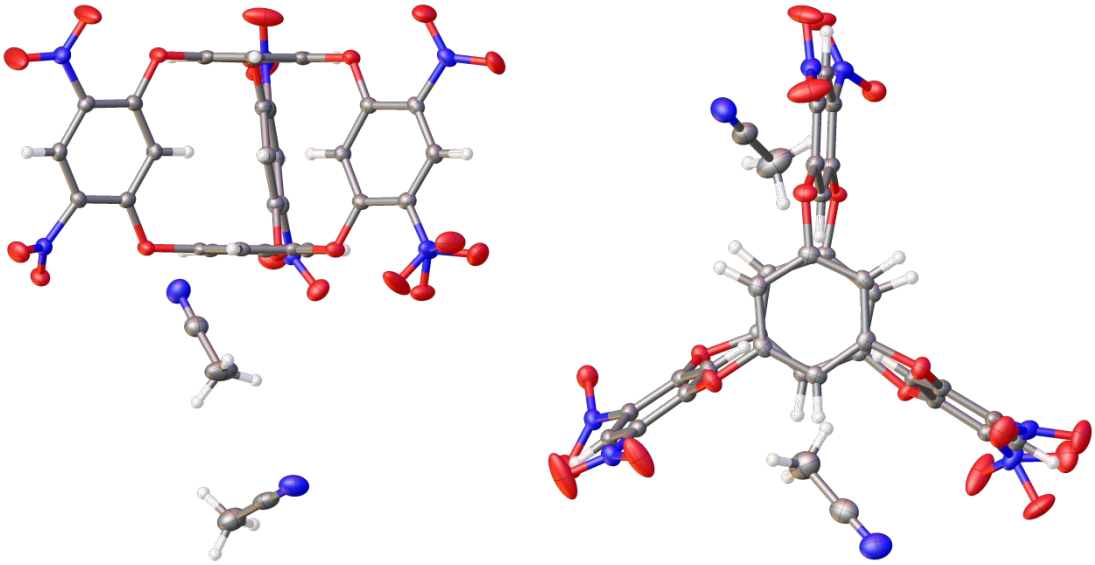

Figure S41. Displacement ellipsoid plots from the single crystal structure of **Cage-6-NO_2**; two views are shown; ellipsoids are displayed at 50% probability level. C = grey; H = white; N = blue; O = red.

Table S4. Single crystal refinement details for **Cage-6-NO_2**.

Name	**Cage-6-NO_2**
Crystallization solvent	acetonitrile, acetone
Wavelength/ Å	Mo-Kα
Formula	$C_{30}H_{12}N_6O_{18}$, $2CH_3CN$
Weight	826.56
Crystal size/mm	0.12 x 0.1 x 0.08
Crystal system	tetragonal
Space group	$I4_1/a$
***a*/ Å**	31.3478(2)
***c*/ Å**	13.70978(16)
***V*/ Å^3**	13472.4(2)
ρ_{calcd}/g cm^{-1}	1.630
Z	16
***T*/K**	100
μ/mm^{-1}	0.136
***F* (000)**	6752
θ range/°	1.62-28.28
Reflections collected	148016
Independent reflections	8357
Obs. Data [$I > 2\sigma$]	6876
Data / restraints / parameters	8357 / 93 / 562
R_{int}	0.0669
Final R_1 values ($I > 2\sigma(I)$)	0.0563
Final R_1 values (all data)	0.0758
wR_2 (all data)	0.1201
Goodness-of-fit on F^2	1.084

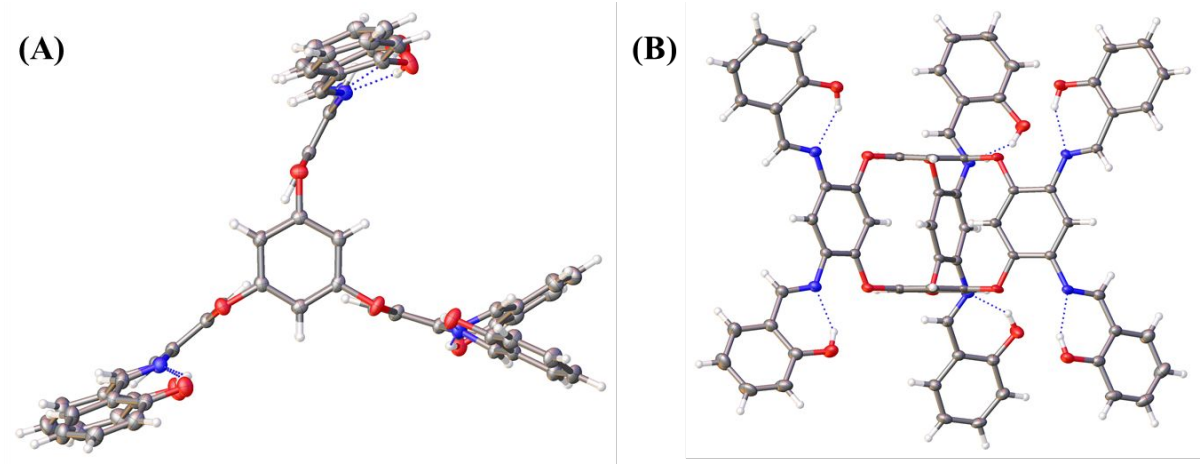

Figure S42. Displacement ellipsoid plots from the single crystal structure of the **Model Compound**; two views are shown; ellipsoids are displayed at 50% probability level. C = grey; H = white; N = blue; O = red.

Table S5. Single crystal refinement details for the **Model Compound**.

Name	**Model Compound**
Crystallization solvent	Toluene, diethyl ether, 1,4-dioxane
Wavelength/ Å	0.6889
Formula	$C_{72}H_{48}N_6O_{12}$, $C_4H_8O_2$, $C_4H_{10}O$, 0.63(C_7H_8)
Weight	1424.97
Crystal size/mm	0.12 x 0.07 x 0.03
Crystal system	triclinic
Space group	$P\bar{1}$
***a*/ Å**	13.89813(6)
***b*/ Å**	15.95700(10)
***c*/ Å**	16.12350(10)
***α*/ °**	87.55
***β*/ °**	85.59
***γ*/ °**	88.55
***V*/ Å^3**	3561.05(4)
ρ_{calcd}/g cm^{-1}	1.329
Z	2
***T*/K**	100
μ/mm^{-1}	0.086
***F* (000)**	1494
***θ* range/°**	1.229- 26.206
Reflections collected	50735
Independent reflections	15557
Obs. Data [$I > 2\sigma$]	11884
Data / restraints / parameters	15557 / 752 / 968
R_{int}	0.0693
Final R_1 values ($I > 2\sigma(I)$)	0.0626
Final R_1 values (all data)	0.0767
wR_2 (all data)	0.2011
Goodness-of-fit on F^2	1.107

Section 12 Atomic Coordinates and Unit Cell Parameters of sp Model and lp Model for 3D-CageCOF-1

Table S6 Atomic coordinates and unit cell parameters of **sp** model for **3D-CageCOF-1**

Name: 3D-CageCOF-1 sp model				
Space Group : $P\ \bar{3}$ (No. 147) ***a* (Å): 19.3698 *c* (Å): 24.4964**				
Atom Name	***x***	***y***	***z***	**Occupancy**
C1	0.7319	0.90183	0.62235	1
C2	0.81242	0.96438	0.62317	1
C3	0.92724	0.99667	0.57312	1
C4	0.99635	0.07076	0.57291	1
C5	0.61058	0.77787	0.12267	1
C6	0.5284	0.71953	0.12386	1
C7	0.41005	0.67911	0.07442	1
C8	0.34624	0.6013	0.07428	1
C9	0.64079	0.75389	0.41628	1
C10	0.65491	0.78559	0.46884	1
C11	0.63657	0.76752	0.31658	1
C12	0.66024	0.80331	0.36993	1
C13	0.68878	0.86965	0.47547	1
C14	0.70874	0.91907	0.4292	1
C15	0.69652	0.88769	0.3766	1
C16	0.70829	0.90595	0.52892	1
C17	0.26749	0.09677	0.27688	1
C18	0.18706	0.03416	0.27837	1
C19	0.07221	0.00185	0.2281	1
C20	0.00223	0.92843	0.22789	1
C21	0.38891	0.22421	0.77639	1
C22	0.47148	0.28142	0.77746	1
C23	0.59004	0.32133	0.728	1
C24	0.65415	0.39897	0.72776	1
C25	0.35802	0.24107	0.06987	1
C26	0.34401	0.21052	0.12271	1
C27	0.36408	0.2273	0.97065	1
C28	0.34274	0.19148	0.02415	1
C29	0.31293	0.12688	0.13007	1
C30	0.2974	0.07724	0.08429	1
C31	0.31163	0.10791	0.0315	1

C32	0.29208	0.0912	0.18363	1
C33	0.17743	0.30559	0.67289	1
C34	0.14286	0.14799	0.67224	1
C35	0.15567	0.35055	0.17316	1
C36	0.20347	0.51165	0.17318	1
O37	0.85359	0.99328	0.57436	1
O38	0.48747	0.69175	0.07494	1
O39	0.63653	0.73687	0.51268	1
O40	0.71795	0.93709	0.33304	1
O41	0.1451	0.00362	0.22988	1
O42	0.51264	0.30906	0.72845	1
O43	0.35897	0.25975	0.16575	1
O44	0.29666	0.05869	0.98841	1
H45	0.99318	0.12523	0.57398	1
H46	0.35623	0.55073	0.07516	1
H47	0.61313	0.68946	0.41119	1
H48	0.65209	0.77294	0.54614	1
H49	0.6035	0.70206	0.31494	1
H50	0.73356	0.98307	0.43466	1
H51	0.69856	0.90112	0.2996	1
H52	0.7364	0.97097	0.53033	1
H53	0.00403	0.87317	0.22949	1
H54	0.64453	0.44973	0.72844	1
H55	0.38116	0.3047	0.06393	1
H56	0.34333	0.22494	0.19958	1
H57	0.39295	0.2926	0.96912	1
H58	0.2725	0.01328	0.09012	1
H59	0.31151	0.09331	0.95457	1
H60	0.26448	0.026	0.18555	1
H61	0.18699	0.36604	0.67329	1
H62	0.12739	0.08562	0.6719	1
H63	0.14068	0.28827	0.17339	1
H64	0.22401	0.57527	0.17318	1
N65	0.65073	0.8104	0.27248	1
N66	0.69523	0.86392	0.57339	1
N67	0.35176	0.18525	0.92633	1
N68	0.30378	0.13362	0.22766	1

Table S7 Atomic coordinates and unit cell parameters of **lp** model for **3D-CageCOF-1**.

Name: 3D-CageCOF-1 lp model				
Space Group : $P\ \bar{3}$ (No. 147) ***a* (Å): 25.47 *c* (Å): 22.93**				
Atom Name	***x***	***y***	***z***	**Occupancy**
C1	0.77814	0.88764	0.62538	1
C2	0.84238	0.92407	0.62687	1
C3	0.93724	0.97082	0.57691	1
C4	0.97032	0.03408	0.57697	1
C5	0.55551	0.77903	0.12527	1
C6	0.49118	0.74263	0.12685	1
C7	0.39614	0.69565	0.07678	1
C8	0.3628	0.63236	0.07677	1
C9	0.61125	0.78165	0.43931	1
C10	0.6519	0.80592	0.48577	1
C11	0.58164	0.78001	0.33635	1
C12	0.62585	0.80714	0.38297	1
C13	0.7101	0.85849	0.47624	1
C14	0.72475	0.88395	0.41981	1
C15	0.68432	0.85933	0.37326	1
C16	0.75338	0.88636	0.52342	1
C17	0.22203	0.1118	0.26527	1
C18	0.15766	0.07552	0.26671	1
C19	0.06276	0.02871	0.21645	1
C20	0.02922	0.96543	0.21643	1
C21	0.44432	0.22112	0.76526	1
C22	0.50871	0.25751	0.76656	1
C23	0.60381	0.30442	0.71637	1
C24	0.6373	0.36773	0.71636	1
C25	0.39138	0.2144	0.08063	1
C26	0.35051	0.19051	0.12692	1
C27	0.41974	0.21802	0.97702	1
C28	0.37557	0.19095	0.02358	1
C29	0.29075	0.14067	0.11641	1
C30	0.27494	0.11717	0.05936	1
C31	0.31578	0.1412	0.01304	1
C32	0.24654	0.11388	0.16303	1
C33	0.12132	0.25086	0.68003	1

C34	0.06819	0.12708	0.68006	1
C35	0.21193	0.41562	0.17998	1
C36	0.26497	0.53924	0.18016	1
O37	0.87405	0.94142	0.57459	1
O38	0.45938	0.72484	0.07474	1
O39	0.63559	0.77975	0.53885	1
O40	0.70073	0.88505	0.31987	1
O41	0.12604	0.05761	0.2146	1
O42	0.5405	0.27531	0.7144	1
O43	0.36786	0.21458	0.18075	1
O44	0.2984	0.11738	0.95905	1
H45	0.94726	0.06037	0.57716	1
H46	0.38557	0.6058	0.07691	1
H47	0.56695	0.74188	0.4475	1
H48	0.67118	0.80543	0.56566	1
H49	0.53797	0.74028	0.34797	1
H50	0.76861	0.92448	0.41189	1
H51	0.66467	0.85977	0.29345	1
H52	0.79652	0.9271	0.51245	1
H53	0.05175	0.93865	0.21681	1
H54	0.6146	0.39435	0.71661	1
H55	0.43669	0.25239	0.08933	1
H56	0.33144	0.18992	0.20701	1
H57	0.46424	0.25617	0.98915	1
H58	0.2296	0.0792	0.05069	1
H59	0.33484	0.14215	0.93291	1
H60	0.20195	0.0758	0.15101	1
H61	0.1415	0.30003	0.68002	1
H62	0.04662	0.07792	0.68014	1
H63	0.19174	0.36646	0.17988	1
H64	0.2865	0.58842	0.18018	1
N65	0.59399	0.80144	0.28327	1
N66	0.74069	0.86462	0.57638	1
N67	0.40645	0.19835	0.92337	1
N68	0.26001	0.13385	0.21657	1

Reference

1. Sheldrick, G. SHELXT. *Acta Cryst.* **2015**, *A7*, 3-8.
2. Sheldrick, G. SHELXL. *Acta Cryst.* **2015**, *C71*, 3-8.
3. Dolomanov, O. V., Bourhis, L. J., Gildea, R. J., Howard, J. A. K. and Puschmann, H. OLEX2. *J. Appl. Cryst.* **2009**, *42*, 339-341.
4. Katz, J. L.; Selby, K. J.; Conry, R. R. A Single-step Synthesis of D_{3h}-Symmetric Bicyclooxacalixarenes. *Org. Lett.* **2005**, *7*, 3505-3507.
5. Sun, Q.; Fu, C. W.; Aguila, B.; Perman, J.; Wang, S.; Huang, H. Y.; Xiao, F. S.; Ma, S. Pore Environment Control and Enhanced Performance of Enzymes Infiltrated in Covalent Organic Frameworks. *J. Am. Chem. Soc.* **2018**, *140*, 984-992.
6. Jagiello, J.; Olivier, J. P. 2D-NLDFT Adsorption Models for Carbon Slit-shaped Pores with Surface Energetical Heterogeneity and Geometrical Corrugation. *Carbon* **2013**, *55*, 70-80.
7. Gao, C.; Li, J.; Yin, S.; Lin, G.; Ma, T.; Meng, Y.; Sun, J.; Wang, C. Isostructural Three-Dimensional Covalent Organic Frameworks. *Angew. Chem. Int. Ed.* **2019**, *58*, 9770-9775.
8. Li, Z.; Li, H.; Guan, X.; Tang, J.; Yusran, Y.; Li, Z.; Xue, M.; Fang, Q.; Yan, Y.; Valtchev, V.; Qiu, S. Three-Dimensional Ionic Covalent Organic Frameworks for Rapid, Reversible, and Selective Ion Exchange. *J. Am. Chem. Soc.* **2017**, *139*, 17771-17774.
9. Ding H.; Li J.; Xie G.; Lin G.; Chen R.; Peng Z.; Yang C.; Wang B.; Sun J.; Wang C. An AIEgen-based 3D Covalent Organic Framework for White Light-Emitting Diodes. *Nat. Commun.* **2018**, *9*, 5234.
10. Zhang, Y.; Duan, J.; Ma, D.; Li, P.; Li, S.; Li, H.; Zhou, J.; Ma, X.; Feng, X.; Wang, B. Three-Dimensional Anionic Cyclodextrin-Based Covalent Organic Frameworks. *Angew. Chem. Int. Ed.* **2017**, *56*, 16313-16317.
11. Chen, Y.; Shi, Z. L.; Wei, L.; Zhou, B.; Tan, J.; Zhou, H. L.; Zhang, Y. B. Guest-Dependent Dynamics in a 3D Covalent Organic Framework. *J. Am. Chem. Soc.* **2019,** *141*, 3298-3303.
12. Lin, G.; Ding, H.; Yuan, D.; Wang, B.; Wang, C. A Pyrene-Based, Fluorescent Three-Dimensional Covalent Organic Framework. *J. Am. Chem. Soc.* **2016,** *138*, 3302-3305.
13. Li, H.; Pan, Q.; Ma, Y.; Guan, X.; Xue, M.; Fang, Q.; Yan, Y.; Valtchev, V.; Qiu, S. Three-Dimensional Covalent Organic Frameworks with Dual Linkages for Bifunctional Cascade Catalysis. *J. Am. Chem. Soc.* **2016**, *138*, 14783-14788.
14. Ma, J. X.; Li, J.; Chen, Y. F.; Ning, R.; Ao, Y. F.; Liu, J. M.; Sun, J.; Wang, D. X.; Wang, Q. Q. Cage Based Crystalline Covalent Organic Frameworks. *J. Am. Chem. Soc.* **2019**, *141*, 3843-3848.
15. Wei, H.; Chai, S.; Hu, N.; Yang, Z.; Wei, L.; Wang, L. The Microwave-Assisted Solvothermal Synthesis of a Crystalline Two-Dimensional Covalent Organic Framework with High CO_2 Capacity. *Chem. Commun.* **2015**, *51*, 12178-12181.
16. Gao, Q.; Li, X.; Ning, G.-H.; Xu, H.-S.; Liu, C.; Tian, B.; Tang, W.; Loh, K. P. Covalent Organic Framework with Frustrated Bonding Network for Enhanced Carbon Dioxide Storage. *Chem. Mater.* **2018**, *30*, 1762-1768.
17. Ozdemir, J.; Mosleh, I.; Abolhassani, M.; Greenlee, L. F.; Beitle, R. R.; Beyzavi, M. H. Covalent Organic Frameworks for the Capture, Fixation, or Reduction of CO_2. *Front. Energy Res.* **2019**, *7*.
18. Guan, X.; Chen, F.; Fang, Q.; Qiu, S. Design and Applications of Three Dimensional Covalent Organic Frameworks. *Chem. Soc. Rev.* **2020**, *49*, 1357-1384
19. Keupp, J.; Schmid, R. TopoFF: MOF Structure Prediction Using Specifically Optimized Blueprints. *Faraday Discuss.* **2018,** *211*, 79-101.